SUPPLEMENTARY INFORMATION

V-shaped D–π–A–π–D molecules based on benzothiophene-S,S-dioxide: tuning of excited states via donor strength to engineer photoactive materials

Mattia Zangoli[a,b,‡], Antonio Maggiore[c,‡], Nicol Spallacci[a], Fabrizio Mariano[c], Filippo Monti[a], Soraia Flammini[a], Marco Pugliese[c], Giuseppe Gigli[d], Vincenzo Maiorano[c], Francesca Di Maria [a,b*]*

[a] CNR-ISOF – Istituto per la Sintesi Organica e la Fotoreattività, via P. Gobetti 101, 40129 Bologna, Italy.
[b] CLAN – Center for Light Activated Nanostructures c/o ISOF-CNR, via P. Gobetti 101, 40129 Bologna, Italy.
[c] CNR-NANOTEC – Institute of Nanotechnology, c/o Campus Ecotekne, Via Monteroni, Lecce, 73100, Italy.
[d] Department of Mathematics and Physics, University of Salento, Via Monteroni, Lecce, 73100, Italy.

I. Reagents and materials.

TLC were carried out with 0.2-mm thick of silica gel 60 F254 (Sigma). Preparative column chromatographies were carried out on glass columns with silica gel 60 (particle sizes 0.040–0.063 mm, Sigma). 2,5-Dibromo-*p*-xylene, Carbazole, Phenoxazine, Phenothiazine, $Pb(dba)_2$, KOAc, Bis(pinacolato)diboron, $PdCl_2(dppf)$ and $[(t\text{-}Bu)_3PH]BF_4$ were purchased from Fluorochem. $CuCO_4$, K_2CO_3, tBuONa, $NiCl_2(dppp)$, 2,3-dibromobenzo[b]thiophene, H_2O_2 (50%), CF_3COOH and $NaHCO_3$ were purchased from Merck. All reagents and solvents were used as received. Organic solvents were dried by standard procedures. Microwave experiments were carried out in a CEM Discover SP-Microwave Synthesizer reactor in a closed vessel (230 W, fixed temperature at 80-90 °C, air, high stirring rate). All ^1H NMR and ^{13}C NMR spectra were recorded on a Varian Mercury-400/500 spectrometer equipped with a 5-mm probe. Chemical shifts were calibrated using the internal $CDCl_3$ resonance, which were referenced to TMS. Mass spectra were collected on a Thermo Scientific TRACE 1300 gas chromatograph.

II. Synthesis

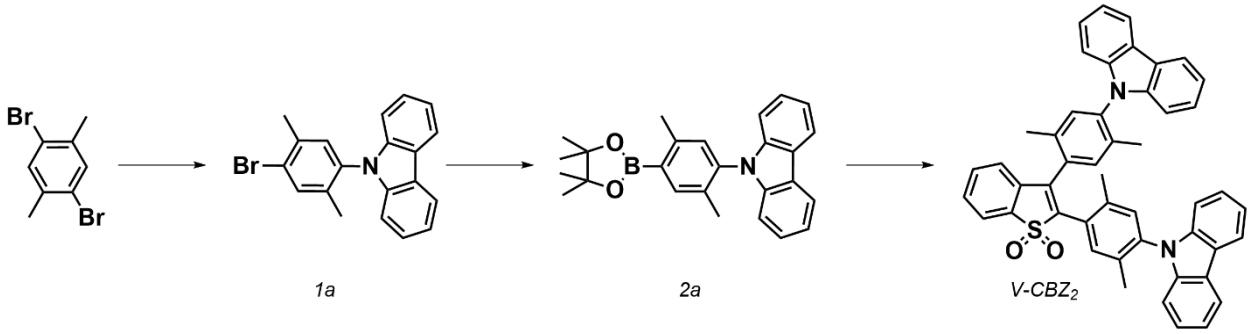

Scheme 1

*9-(4-bromo-2,5-dimethylphenyl)-9H-carbazole (**1a**)* → carbazole (1 mmol), 2,5-dibromo-*p*-xylene (2.5 mmol), dry $CuSO_4$ (0.8 mmol), and K_2CO_3 (2 mmol) were heated to 210 °C overnight inside a capped flask, in solvent-free conditions and nitrogen atmosphere. Then, the mixture was cooled to room temperature and extracted three times with CH_2Cl_2/H_2O. The organic phases were combined, and the pure product was isolated by flash chromatography (cyclohexane 100%) as a colorless solid (55% yield). EI-MS: m/z 349 (M^+). ^1H-NMR (500 MHz, $CDCl_3$, TMS/ppm): 8.18 (d, 2H, J = 8 Hz), 7.69 (s, 1H), 7.44-7.41 (m, 2H), 7.32-7-29 (m, 2H), 7.26 (s, 1H), 7. 07 (d, 2H, J = 8.5 Hz), 2.45 (s, 3H), 1.95 (s, 1H). ^{13}C-NMR (126 MHz, $CDCl_3$, TMS/ppm): 140.9, 137.0, 136.6, 135.2, 134.9, 131.2,125.9, 124.8, 123.1, 120.4, 119.7, 109.7, 22.5, 16.9.
*9-(2,5-dimethyl-4-(4,4,5,5-tetramethyl-1,3,2-dioxaborolan-2-yl)phenyl)-9H-carbazole (**2a**)* → ***1a*** (1 mmol), bis(pinacolato)diboron (1.2 mmol), and KOAc (1.5 mmol) were dissolved in freshly distilled 1,4-dioxane, and the resulting mixture was flushed with N_2 for 15 min. Thereafter, $Pd(dppf)Cl_2$ (5% mmol) was added, and the final solution was refluxed at 100°C overnight. Afterward, the solvent was removed under reduced pressure, and the final residue was extracted three times with CH_2Cl_2/H_2O. The resulting organic phases were combined, and the pure product was isolated by flash chromatography (cyclohexane/CH_2Cl_2, 80/20) as a white solid (70% yield).

EI-MS: m/z 397 (M^+). ^{1}H-NMR (500 MHz, $CDCl_3$, TMS/ppm): 8.24 (d, 2H, *J* = 7.5 Hz), 8.00 (s, 1H), 7.48-7.45 (m, 2H), 7.37-7.24 (m, 2H), 7.28 (s, 1H), 7. 16 (d, 2H, *J* = 8.5 Hz), 2.68 (s, 3H), 2.06 (s, 1H), 1.49 (s, 12H). ^{13}C-NMR (126 MHz, $CDCl_3$, TMS/ppm): 144.1, 141.1, 139.1, 138.2, 133.2, 130.3, 125.9, 123.1, 120.4, 119.6, 109.9, 83.8, 25.0, 21.8, 17.1.

*2,3-bis(4-(9H-carbazol-9-yl)-2,5-dimethylphenyl)benzo[b]thiophene 1,1-dioxide (**V-CBZ$_2$**)* → 2,3-dibromobenzo[b]thiophene 1,1-dioxide (1mmol), ***2a*** (2.2 mmol), $NaHCO_3$ (6 mmol) and Pd(dppf)Cl_2 (5% mmol) were dissolved in THF/H_2O (2/1), and the resulting mixture was heated to 90°C through microwave irradiation for 30 min. Thereafter, the reaction mixture was extracted three times with CH_2Cl_2/H_2O, and the organic phases were combined. The crude product was purified through flash chromatography (cyclohexane/CH_2Cl_2/AcOEt, 75/25/5) giving a white powder (60% yield). EI-MS: m/z 704 (M^+). ^{1}H-NMR (500 MHz, $CDCl_3$, TMS/ppm): 8.20-8.16 (m, 4H), 7.99 (d, 1H, *J* = 7.5 Hz), 7.70-7.65 (m, 3H), 7.48-7.45 (m, 1H), 7.42-7.29 (m, 11H), 7.16 (d, 1H, *J* = 8 Hz), 7.04 (d, 2H, *J* = 8 Hz), 6.91 (d, 1H, *J* = 8 Hz), 2.38 (s, 3H), 2.31 (s, 3H), 2.02 (s, 3H), 1.98 (s, 3H). ^{13}C-NMR (126 MHz, $CDCl_3$, TMS/ppm): 140.9, 140.87, 140.84, 140.3, 139.2, 138.0, 137.7, 137.2, 136.5, 135.5, 135.1, 134.8, 133.9, 133.7, 132.7, 132.1, 131.5, 131. 2, 130.7, 130.5, 126.4, 126.2, 126.1, 126.0, 125.9, 124.3, 123.2, 123.19, 123.15, 121.9, 120.5, 120.4, 119.9, 119.8, 119.7, 109.6, 109.3, 19.9, 19.8, 17.3, 17.2.

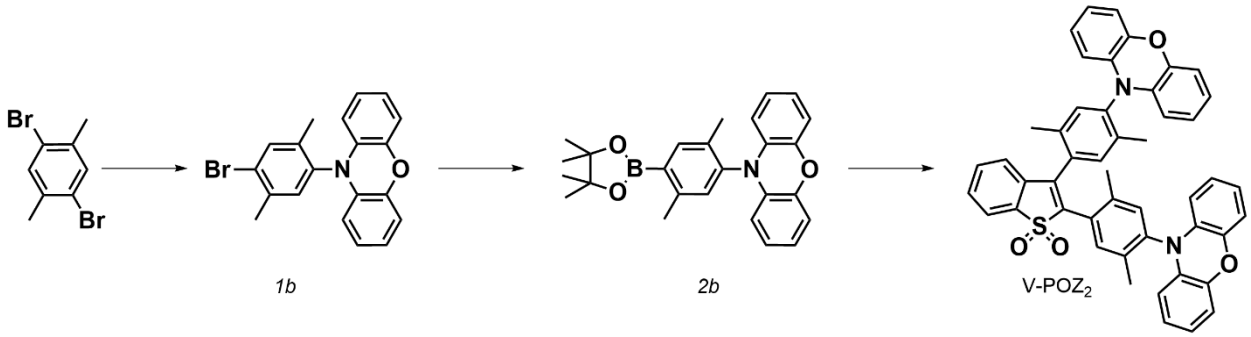

Scheme 2

*10-(4-bromo-2,5-dimethylphenyl)-10H-phenoxazine (**1b**)* → phenoxazine (1mmol), 2,5-dibromo-*p*-xylene (3 mmol), and Ni(dppf)Cl_2 were dissolved in dry toluene, and the resulting mixture was bubbled with an inert atmosphere for 15 min. Then, 1.4 mmol of freshly prepared EtMgBr (1M in MeTHF) was added dropwise under N_2 atmosphere. As the Grignard reagent was added, the solution started immediately to bubble and in a few minutes turned from red/orange to a deep green color. After 10 min of magnetic stirring, the reaction mixture was refluxed at 110°C for 8 h. The reaction was quenched with an aqueous solution of $NH_4Cl_{(sat)}$, the resulting mixture was extracted twice with CH_2Cl_2/H_2O, and the organic phases combined. The crude product was purified through flash chromatography (cyclohexane, 100%), giving a white solid (30% yield). EI-MS: m/z 365 (M^+). ^{1}H-NMR (500 MHz, $CDCl_3$, TMS/ppm): 7.64 (s, 1H), 7.17 (s, 1H), 6.71-6.59 (m, 6H), 5.82 (d, 2H, *J* = 7.6 Hz), 2.42 (s, 3H), 2.20 (s, 3H). ^{13}C-NMR (126 MHz, $CDCl_3$, TMS/ppm): 143.8, 138.4, 135.7, 133.1, 132.9, 124.9, 123.4, 121.3, 115.5, 112.6, 22.5, 16.9.

*10-(2,5-dimethyl-4-(4,4,5,5-tetramethyl-1,3,2-dioxaborolan-2-yl)phenyl)-10H-phenoxazine (**2b**)* → ***1b*** (1 mmol), bis(pinacolato)diboron (1.2 mmol), and KOAc (1.5 mmol) were dissolved in freshly distilled 1,4-dioxane, and the resulting mixture was flushed with N_2 for 15 min. Pd(dppf)Cl_2 (5% mmol) was added, and the final solution was refluxed to 100°C overnight. The solvent was removed under reduced pressure, and the residue was extracted three times with CH_2Cl_2/H_2O. The organic phases were combined, and the pure product was isolated by flash

chromatography (cyclohexane/CH_2Cl_2, 80/20) as a greenish solid (75% yield). EI-MS: m/z 413 (M^+). ^{1}H-NMR (500 MHz, $CDCl_3$, TMS/ppm): 7.87 (s, 1H), 7.11 (s, 1H), 6.71-6.57 (m, 6H), 5.82 (d, 2H, *J* = 6.4 Hz), 2.58 (s, 3H), 2.23 (s, 3H), 1.43 (s, 12H). ^{13}C-NMR (126 MHz, $CDCl_3$, TMS/ppm):145.4, 143.8, 139.6, 138.9, 134.8, 133.3, 131.8, 123.4, 121.1, 115.3, 112.7, 83.7, 24.9, 21.7, 16.9.

*2,3-bis(2,5-dimethyl-4-(10H-phenoxazin-10-yl)phenyl)benzo[b]thiophene 1,1-dioxide (**V-POZ$_2$**)* → 2,3-dibromobenzo[b]thiophene 1,1-dioxide (1mmol), ***2b*** (2.2 mmol), $NaHCO_3$ (6 mmol) and Pd(dppf)Cl_2 (5% mmol) were dissolved in THF/H_2O (2/1), and the resulting mixture was irradiated with microwave to 90°C for 30 min. The solution was extracted three times with CH_2Cl_2/H_2O and the organic phases combined. The crude product was purified through flash chromatography (cyclohexane/CH_2Cl_2, 70/30) giving a yellowish solid (50% yield). EI-MS: m/z 736 (M^+). ^{1}H-NMR (500 MHz, $CDCl_3$, TMS/ppm): 7.96-7.95 (m, 1H), 7.67-7.63 (m, 2H), 7.59 (s, 1H), 7.24-7.20 (m, 3H),7.15 (s, 1H), 6.72-6.38 (m, 12H), 5.85 (d, 2H, *J* = 6 Hz), 5.70 (d, 1H, *J* = 7 Hz), 5.64 (d, 1H, *J* = 6.5 Hz), 5.46 (d, 1H, *J* = 8 Hz), 2.29 (s, 3H), 2.25 (s, 3H), 2.22 (s, 3H), 2.15 (s, 3H). ^{13}C-NMR (126 MHz, $CDCl_3$, TMS/ppm):143.7, 140.5, 139.3, 139.2, 138.4, 138.0, 136.9, 136.8, 136.5, 136.48, 134.6, 133.7, 133.3, 132.99, 132.9, 132.8, 132.4, 130.8, 130.5, 126.6, 124.3, 123.8, 123.6, 123.4, 121.98, 121.5, 121.4, 121.3, 115.6, 115.4, 112.4, 112.2, 111.8, 19.99, 19.7, 17.0, 16.9.

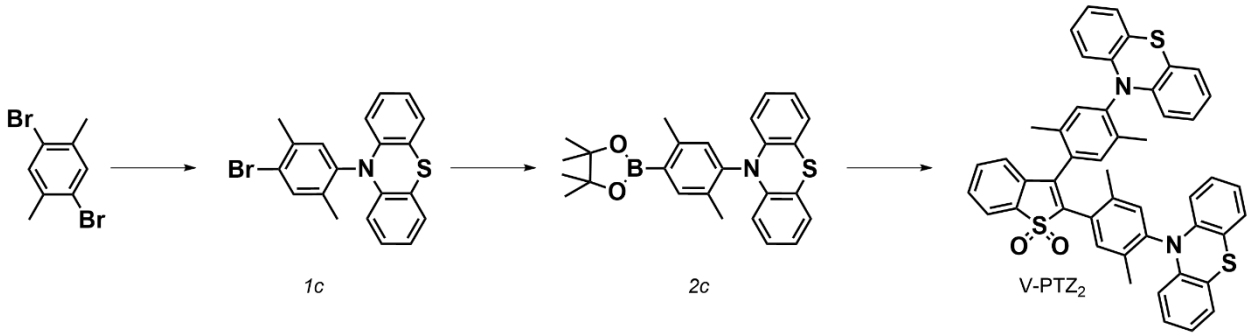

Scheme 3

*10-(4-bromo-2,5-dimethylphenyl)-10H-phenothiazine (**1c**)* → phenothiazine (1 mmol), 2,5-dibromo-*p*-xylene (3 mmol), *t*BuONa (3 mmol), $Pd(dba)_2$ (3% mmol) and tri-*tert*-butylphosphine tetrafluoroborate (3% mmol) were dissolved in dry toluene under nitrogen atmosphere, and the resulting mixture was refluxed at 110 °C overnight. Afterwards, the solvent was evaporated under reduced pressure and the final residue was purified through flash chromatography (cyclohexane/CH_2Cl_2, 90/10) obtaining a white solid (40 % yield). EI-MS: m/z 381 (M^+). ^{1}H-NMR (500 MHz, $CDCl_3$, TMS/ppm): 7.68 (s, 1H), 7.24 (s, 1H), 6.99-6.55 (m, 6H), 6.03 (s, 2H), 2.46 (s, 3H), 2.19 (s, 3H). ^{13}C-NMR (126 MHz, $CDCl_3$, TMS/ppm): 138.1, 135.8, 127.0, 124.8, 114.8, 22.6, 17.1.

*10-(2,5-dimethyl-4-(4,4,5,5-tetramethyl-1,3,2-dioxaborolan-2-yl)phenyl)-10H-phenothiazine (**2c**)* → ***1c*** (1 mmol), bis(pinacolato)diboron (1.2 mmol) and KOAc (1.5 mmol) were dissolved in freshly distilled 1,4-dioxane, and the resulting mixture was bubbled with N_2 for 15 min. After this time, Pd(dppf)Cl_2 (5% mmol) was added, and the final solution was refluxed at 100°C overnight. Then, the solvent was removed under reduced pressure and the resulting residue was extracted three times with CH_2Cl_2/H_2O. The organic phases were combined and the pure product was isolated by flash chromatography (cyclohexane/CH_2Cl_2, 80/20) as a pink solid (85% yield). EI-

MS: m/z 429 (M^+). ^{1}H-NMR (500 MHz, $CDCl_3$, TMS/ppm): 7.89 (s, 1H), 7.15 (s, 1H), 6.97-6.40 (m, 6H), 5.99 (s, 2H), 2.59 (s, 3H), 2.19 (s, 3H), 1.42 (s, 12H). ^{13}C-NMR (126 MHz, $CDCl_3$, TMS/ppm): 145.1, 139.7, 126.9, 114.9, 83.7, 24.9, 21.7, 17.0.

*2,3-bis(2,5-dimethyl-4-(10H-phenothiazin-10-yl)phenyl)benzo[b]thiophene 1,1-dioxide (**V-PTZ$_2$**)* → 2,3-dibromobenzo[b]thiophene 1,1-dioxide (1mmol), ***2c*** (2.2 mmol), $NaHCO_3$ (6 mmol) and $Pd(dppf)Cl_2$ (5% mmol) were dissolved in THF/H_2O (2/1), and the resulting mixture was heated to 90°C through microwave irradiation for 30 min. The solution was extracted three times with CH_2Cl_2/H_2O and the organic phases combined. The crude product was purified through flash chromatography (cyclohexane/CH_2Cl_2/AcOEt, 90/5/5) giving a yellowish solid (80% yield). EI-MS: m/z 768 (M^+). ^{1}H-NMR (500 MHz, $CDCl_3$, TMS/ppm): 7.97-7.95 (m, 1H), 7.68-7.64 (s, 3H), 7.29-7.20 (m, 4H), 6.98-6.45 (m, 12H), 5.88 (s, 4H) 2.31 (s, 3H), 2.29 (s, 3H), 2.21 (s, 3H), 2.13 (s, 3H). ^{13}C-NMR (126 MHz, $CDCl_3$, TMS/ppm): 140.6, 139.2, 138.9, 136.5, 134.8, 133.6, 133.0, 132.3, 130.6, 130.5, 127.2, 126.5, 124.4, 121.9, 114.6, 114.3, 20.1, 19.8, 17.2, 17.1.

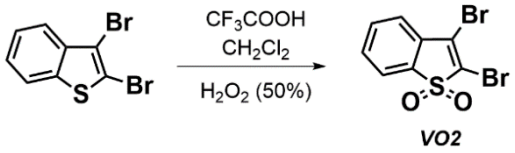

Scheme 4

*dibromobenzo[b]thiophene 1,1-dioxide (**VO$_2$**)* → to a solution of dibromobenzo[b]thiophene (1mmol) in CH_2Cl_2/CF_3COOH (2/1), H_2O_2 (50%) was added dropwise under magnetic stirring. TLC monitoring revealed that in 10-15 min the reagent was completely consumed and the reaction mixture was neutralized with a solution $NaHCO_{3(sat)}$. Then, the mixture was repeatedly extracted with CH_2Cl_2/$NaHCO_{3(sat)}$ until the bubbling definitely disappeared. Finally, the crude product was purified through a filtration on a silica plug (cyclohexane/AcOEt, 60/40) giving a pure product as a white powder (95%). EI-MS: m/z 322 (M^+). ^{1}H-NMR (500 MHz, $CDCl_3$, TMS/ppm): 7.77-7.74 (m, 1H), 7.69-7.65 (m, 1H), 7.61-7.57 (m, 2H). ^{13}C-NMR (126 MHz, $CDCl_3$, TMS/ppm): 135.6, 134.2, 131.4, 130.9, 128.6, 124.4, 123.3, 121.7.

Table S1. General reaction scheme for **D**-coupling reaction optimization. Results are reported as isolated yields.

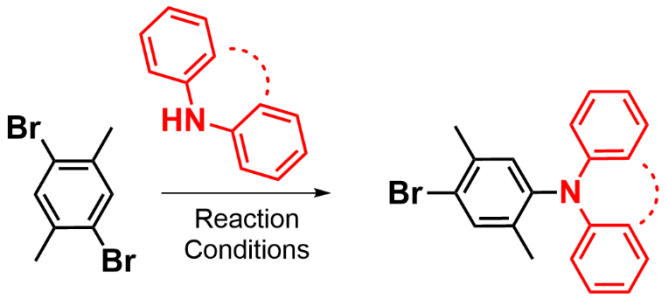

Reaction Conditions **1**: $CuCO_4$, K_2CO_3, 200°C, overnight
Reaction Conditions **2**: EtMgBr, $NiCl_2$(dppp), Toluene,110°C, overnight
Reaction Conditions **3**: *t*BuONa, $Pb(dba)_2$, $[(t\text{-}Bu)_3PH]BF_4$, Toluene, 110°C, overnight

	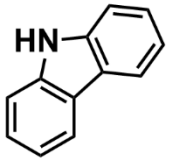	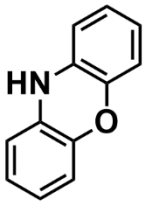	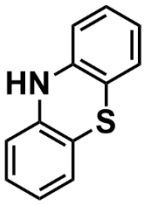
Reaction Conditions **1**	55 %*	< 5 %*	< 5 %*
Reaction Conditions **2**	No product	30 %*	15 %*
Reaction Conditions **3**	20 %*	10 %*	40 %*

* = isolated yields

III. ^{1}H- and ^{13}C-NMR spectra

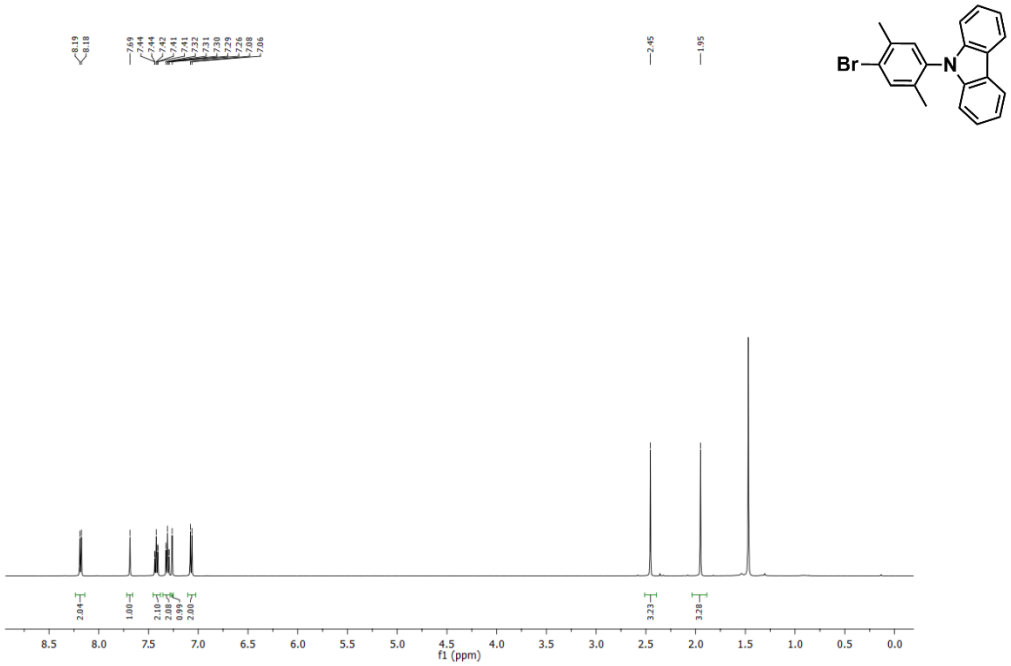

Figure S1. ^{1}H NMR spectrum of compound ***1a*** ($CDCl_3$, 500 MHz, 298.15 K).

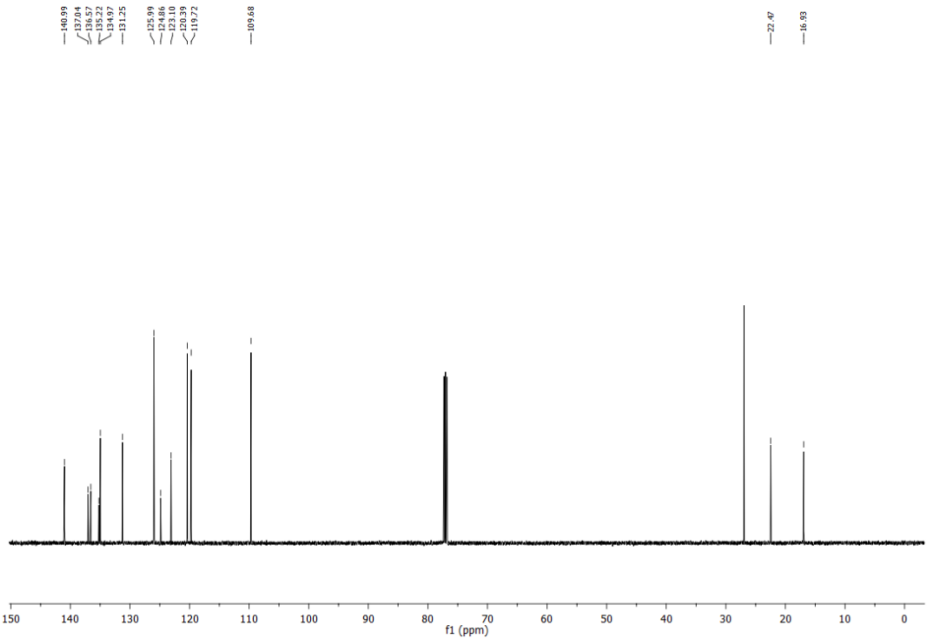

Figure S2. ^{13}C NMR spectrum of compound ***1a*** ($CDCl_3$, 126 MHz, 298.15 K).

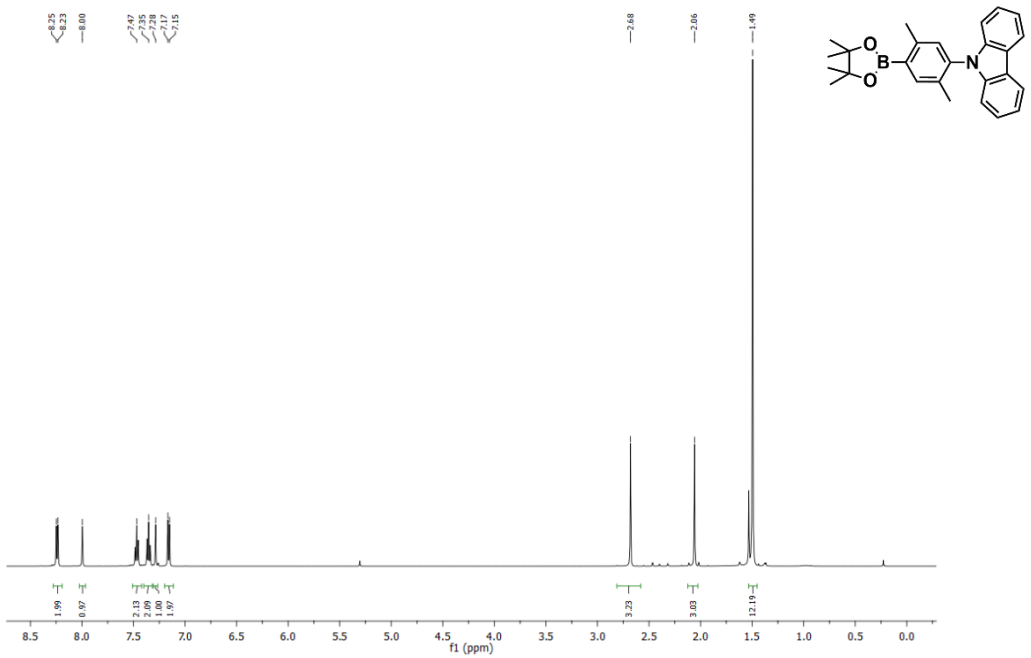

Figure S3. ^{1}H NMR spectrum of compound 2***a*** ($CDCl_3$, 500 MHz, 298.15 K).

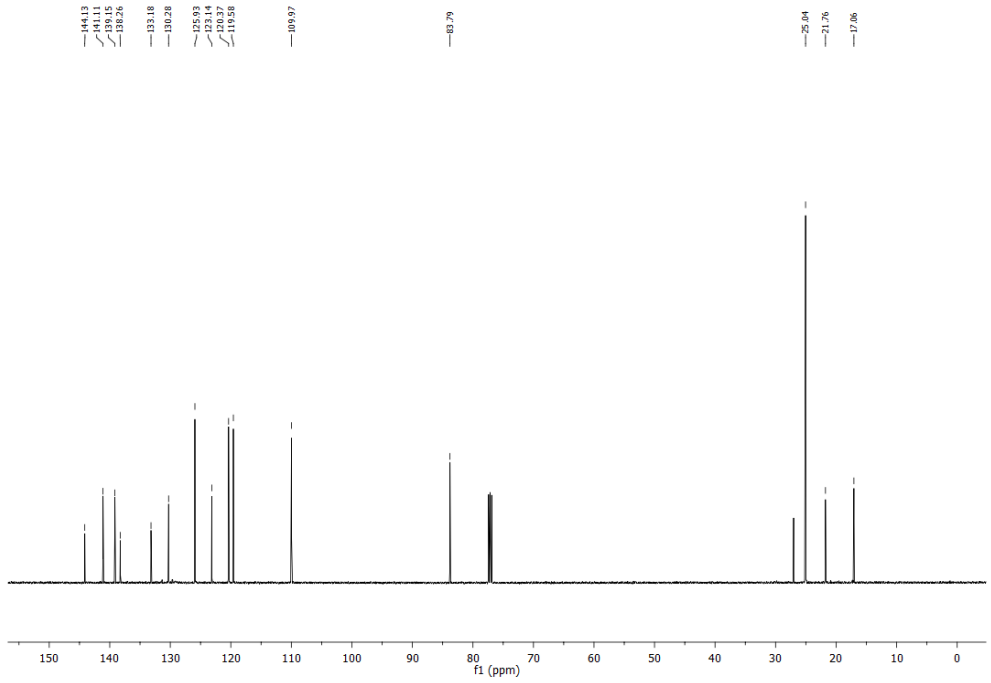

Figure S4. ^{13}C NMR spectrum of compound ***2a*** ($CDCl_3$, 126 MHz, 298.15 K).

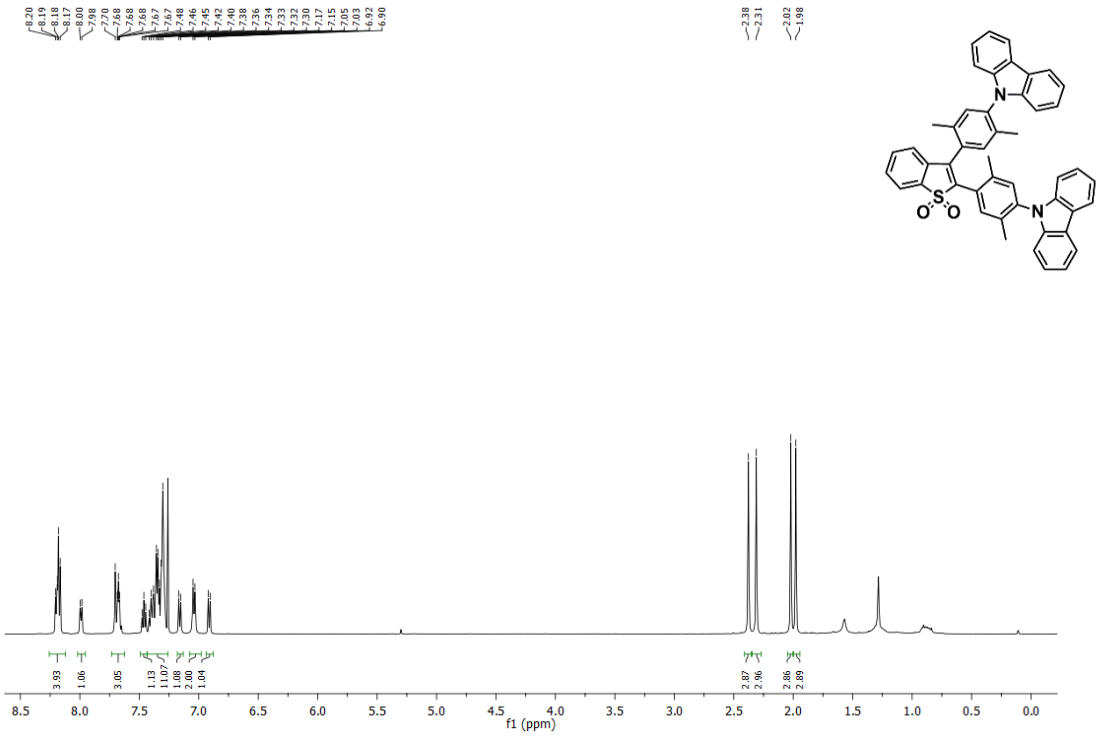

Figure S5. ^{1}H NMR spectrum of compound **V-CBZ$_2$** ($CDCl_3$, 500 MHz, 298.15 K).

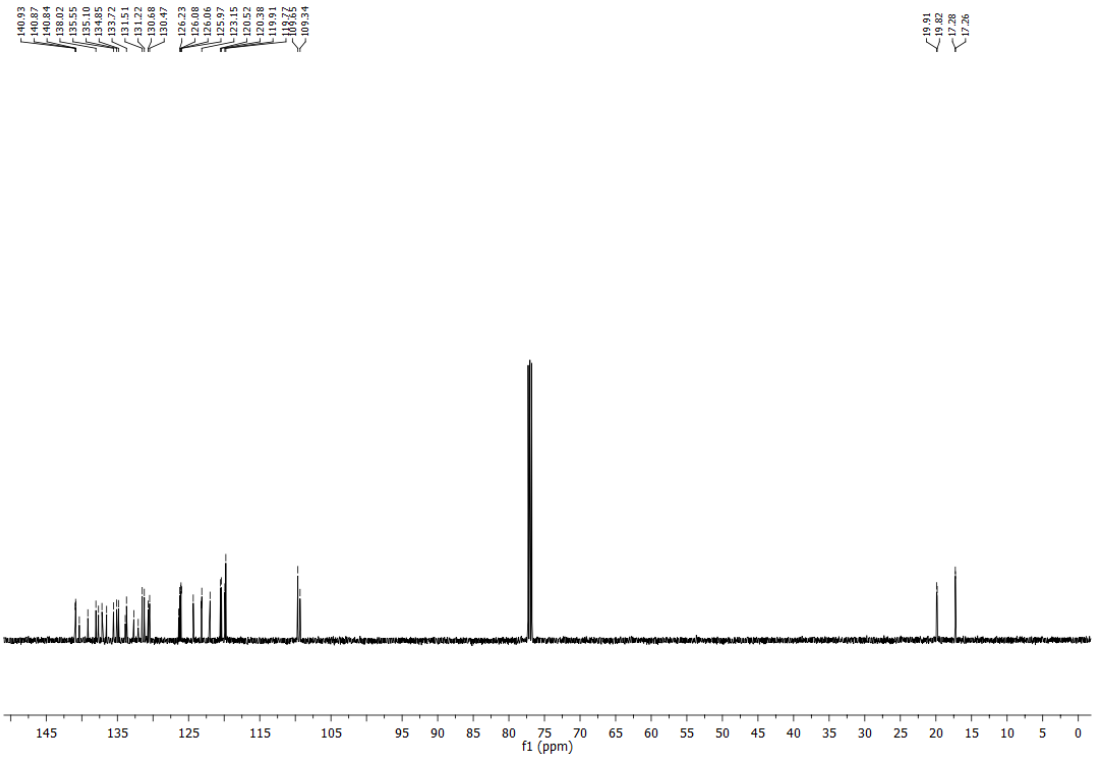

Figure S6. ^{13}C NMR spectrum of compound **V-CBZ$_2$** ($CDCl_3$, 126 MHz, 298.15 K).

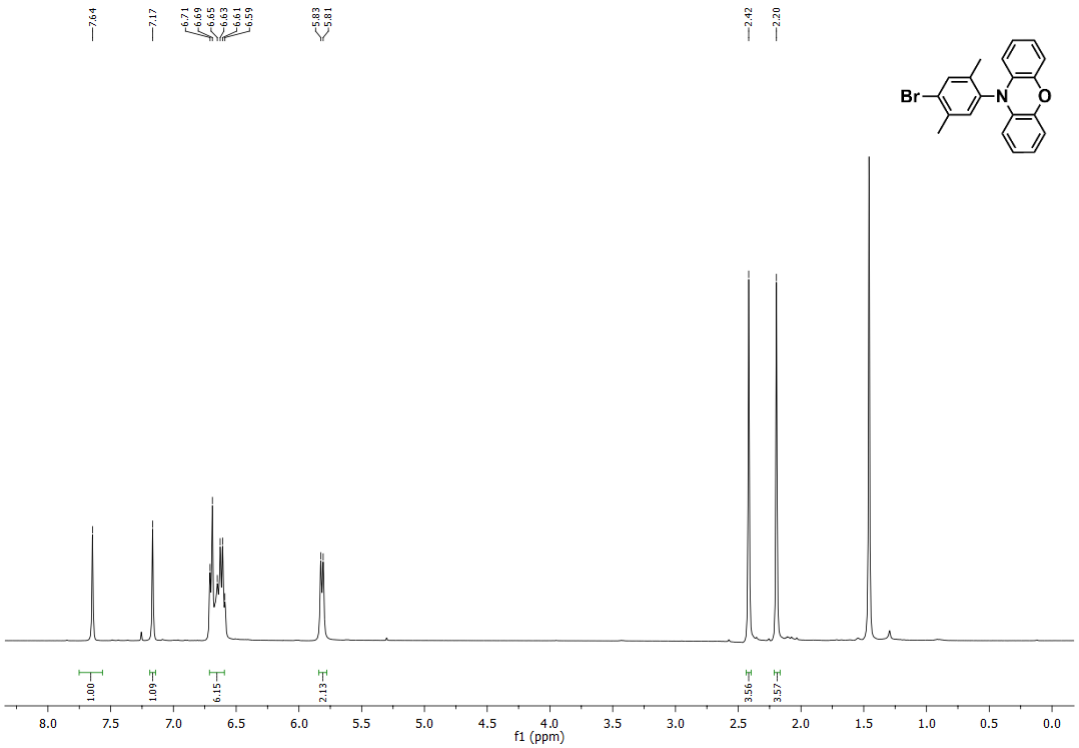

Figure S7. ^{1}H NMR spectrum of compound ***1b*** ($CDCl_3$, 500 MHz, 298.15 K).

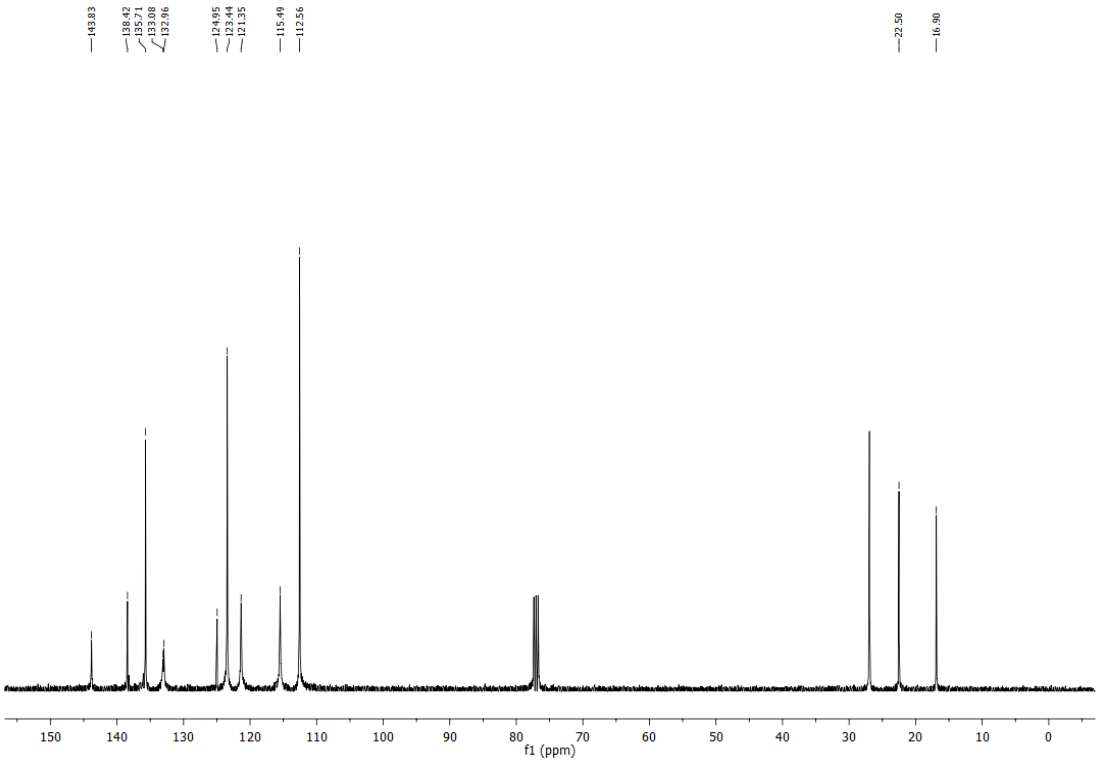

Figure S8. ^{13}C NMR spectrum of compound ***1b*** ($CDCl_3$, 126 MHz, 298.15 K).

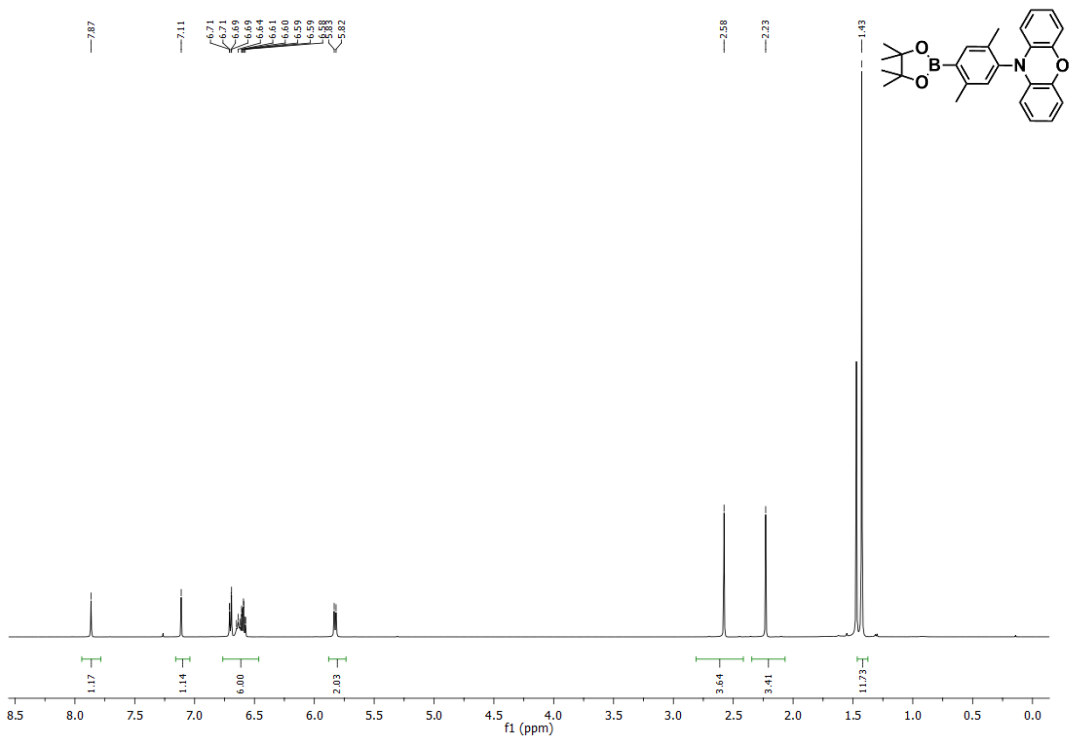

Figure S9. ^{1}H NMR spectrum of compound ***2b*** ($CDCl_3$, 500 MHz, 298.15 K).

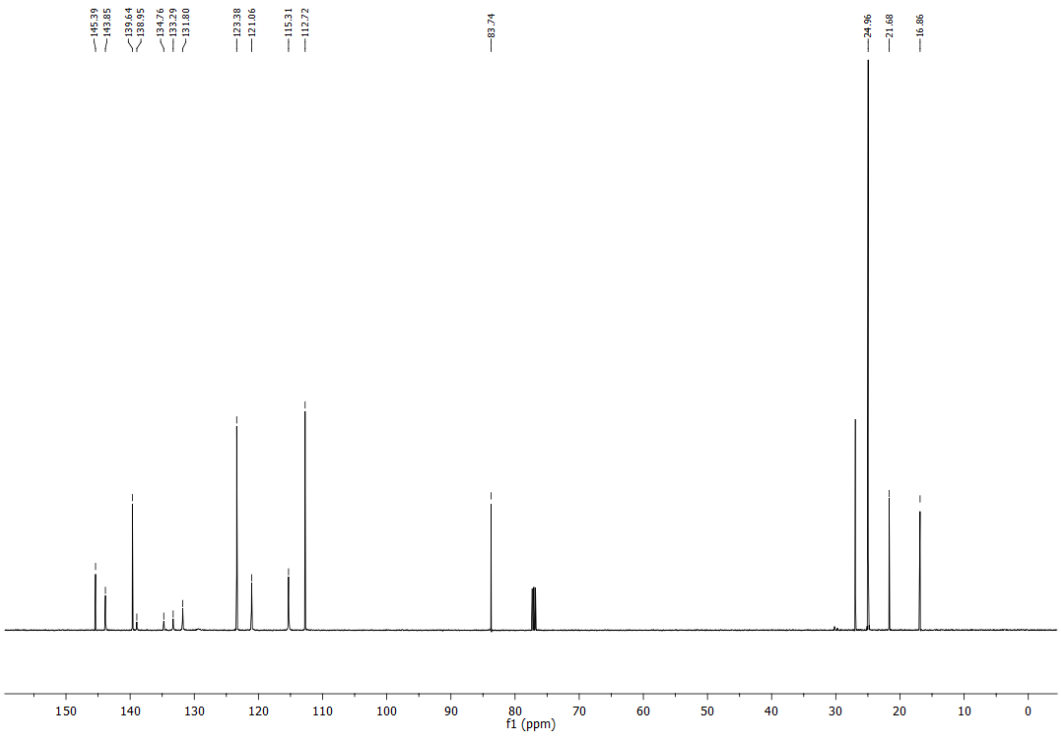

Figure S10. ^{13}C NMR spectrum of compound ***2b*** ($CDCl_3$, 126 MHz, 298.15 K).

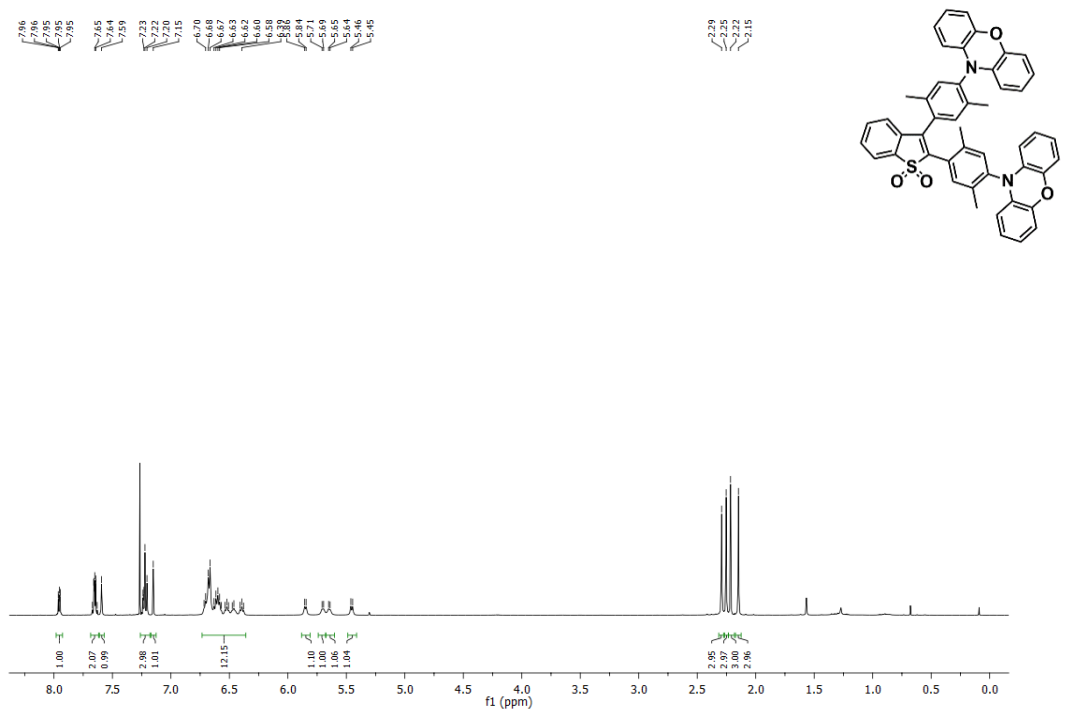

Figure S11. ^{1}H NMR spectrum of compound **V-POZ$_2$** ($CDCl_3$, 500 MHz, 298.15 K).

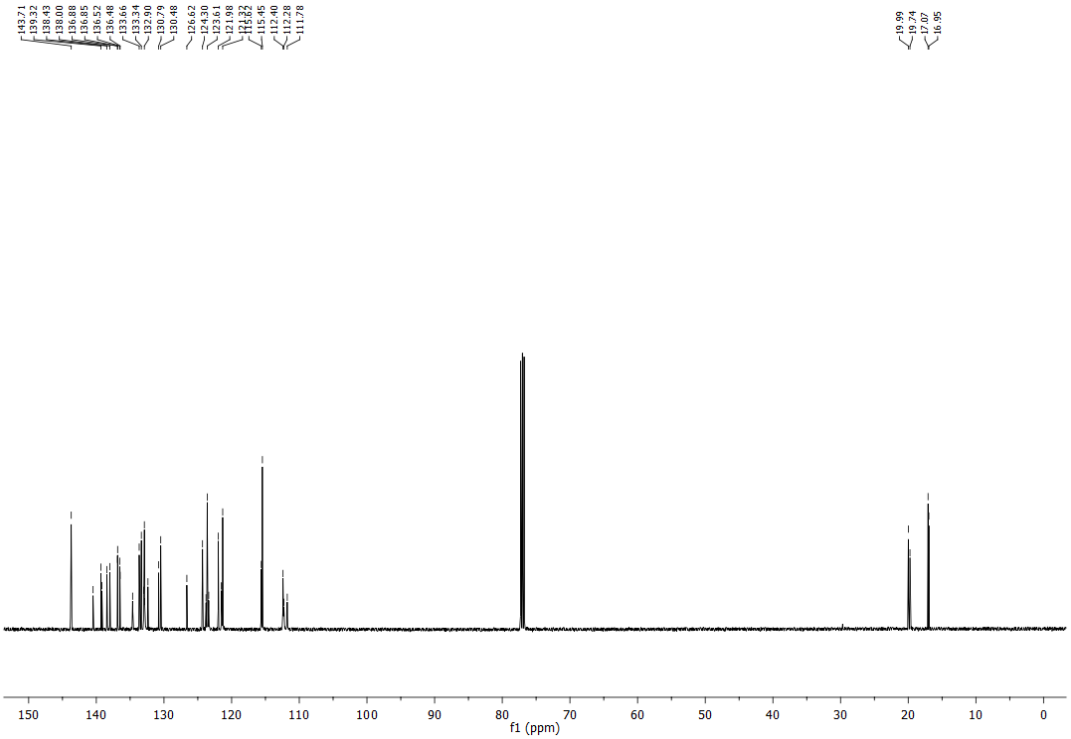

Figure S12. ^{13}C NMR spectrum of compound **V-POZ$_2$** ($CDCl_3$, 126 MHz, 298.15 K).

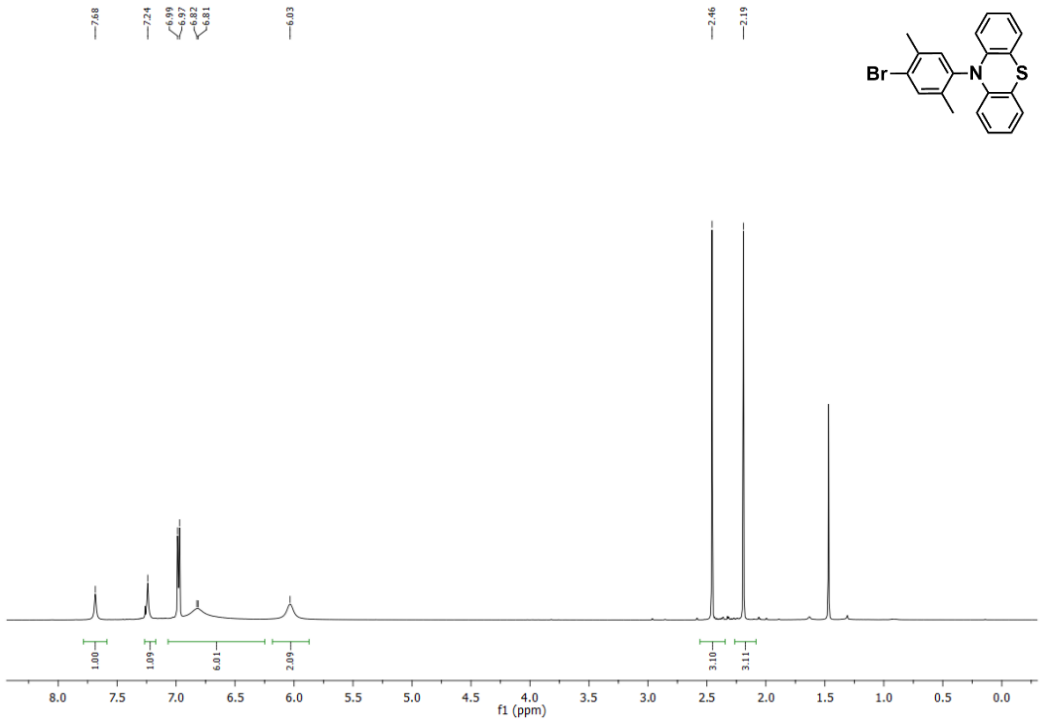

Figure S13. ^{1}H NMR spectrum of compound ***1c*** ($CDCl_3$, 500 MHz, 298.15 K).

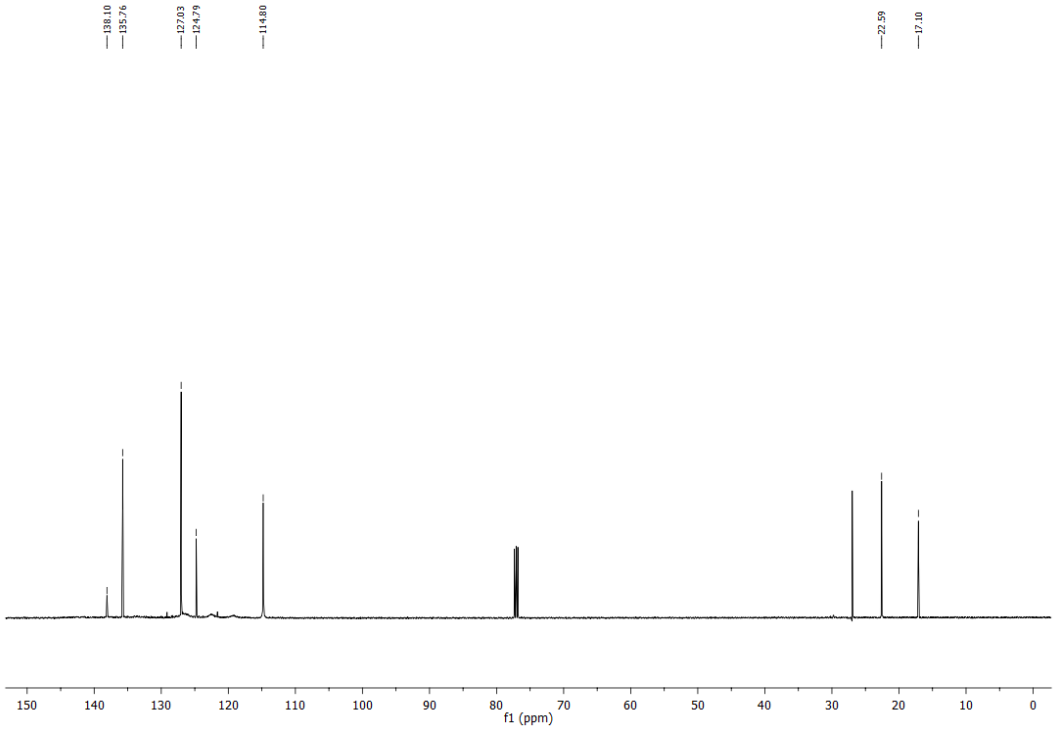

Figure S14. ^{13}C NMR spectrum of compound ***1c*** ($CDCl_3$, 126 MHz, 298.15 K).

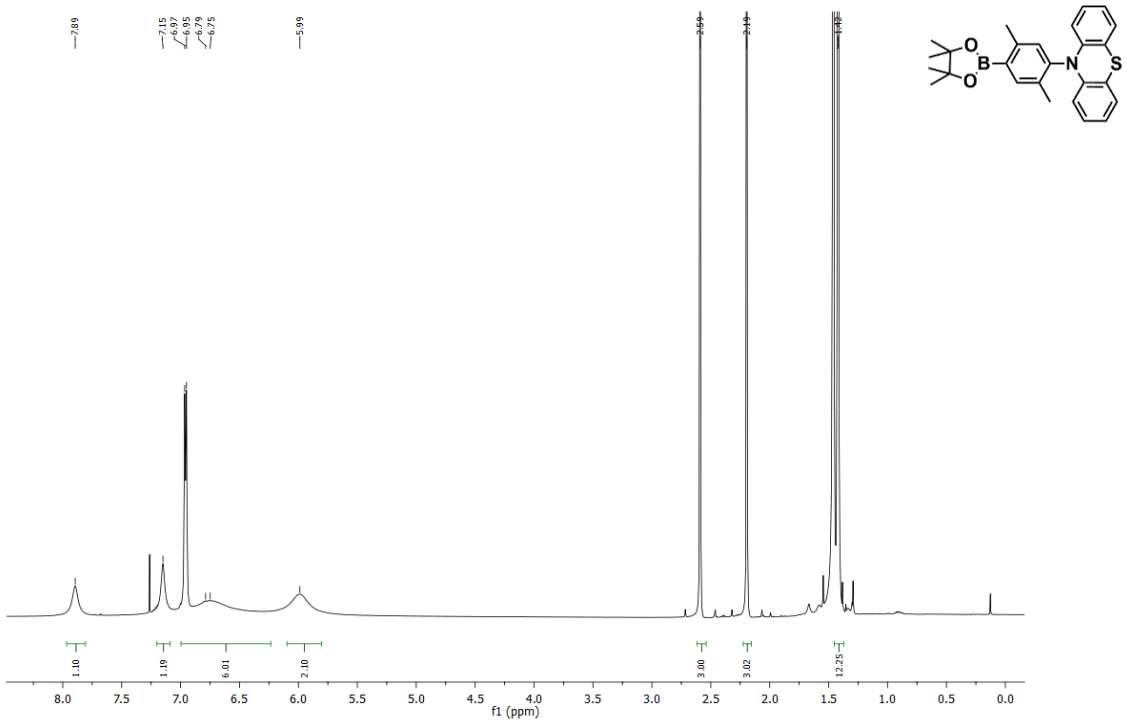

Figure S15. ^{1}H NMR spectrum of compound ***2c*** ($CDCl_3$, 500 MHz, 298.15 K).

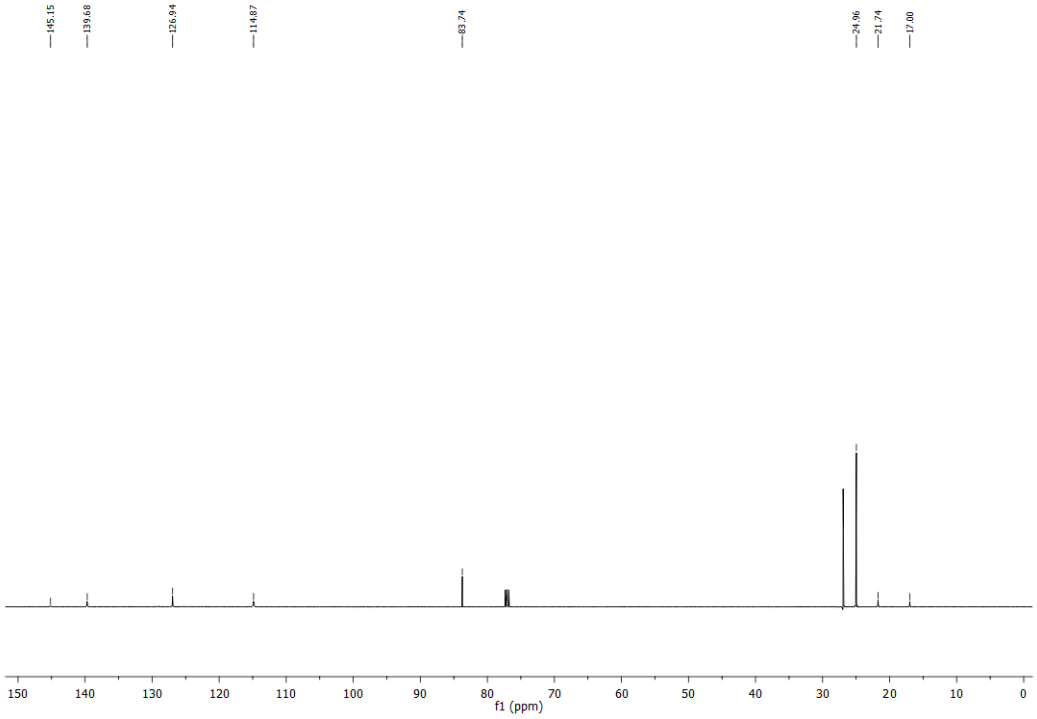

Figure S16. ^{13}C NMR spectrum of compound ***2c*** ($CDCl_3$, 126 MHz, 298.15 K).

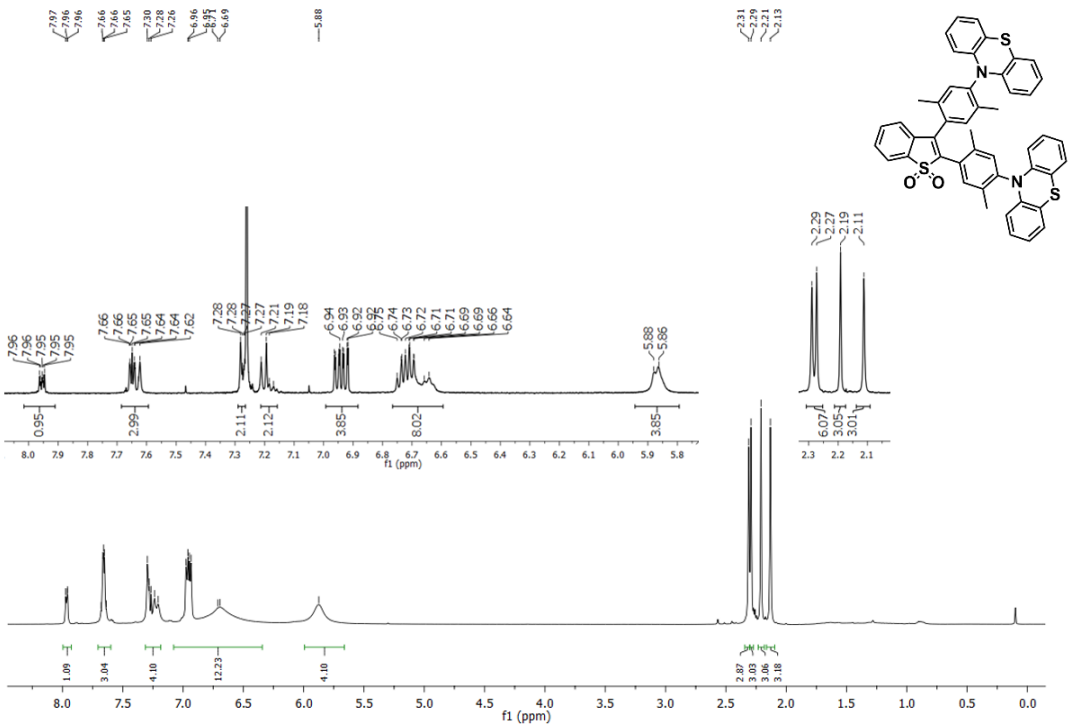

Figure S17. ^{1}H NMR spectrum of compound **V-PTZ$_2$** at two different concentrations: main spectrum at 0.5 mM and expanded region at 0.02 mM ($CDCl_3$, 500 MHz, 298.15 K).

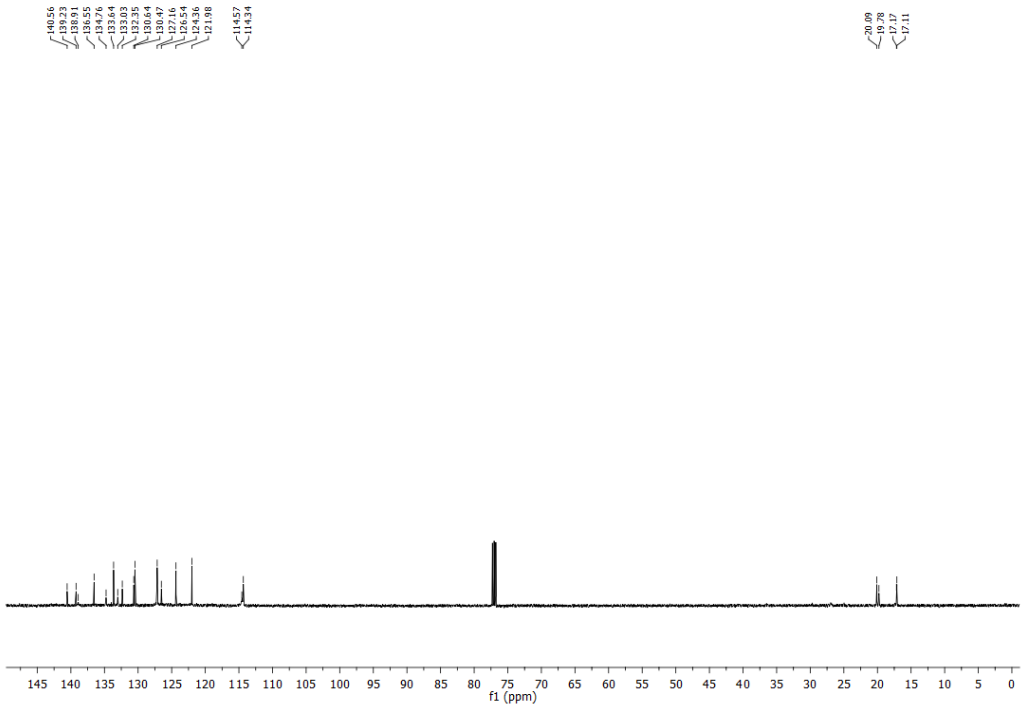

Figure S18. ^{13}C NMR spectrum of compound **V-PTZ$_2$** ($CDCl_3$, 126 MHz, 298.15 K).

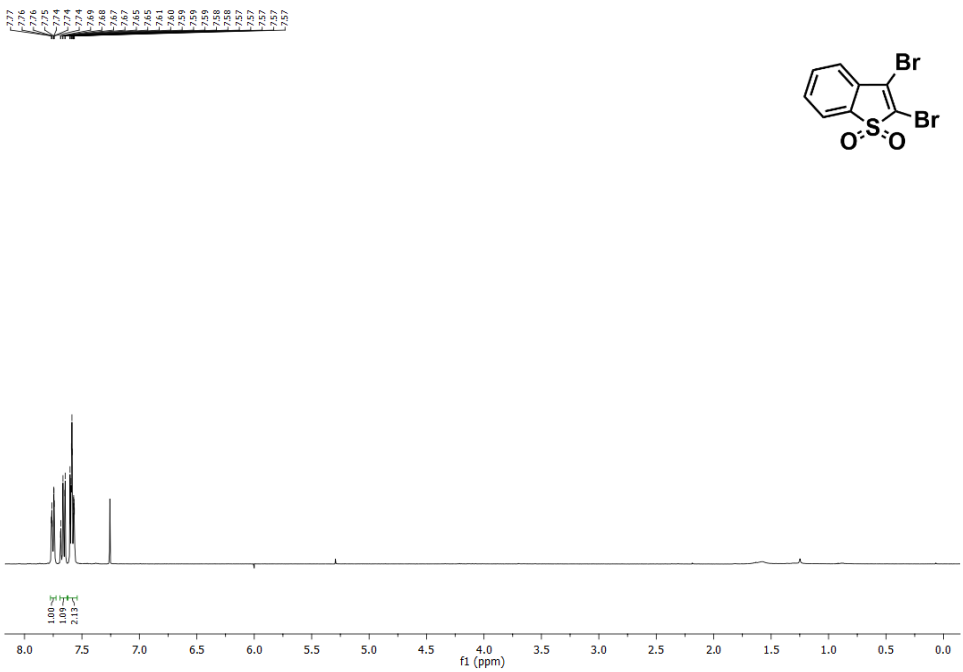

Figure S19. ^{1}H NMR spectrum of compound ***VO₂*** ($CDCl_3$, 500 MHz, 298.15 K).

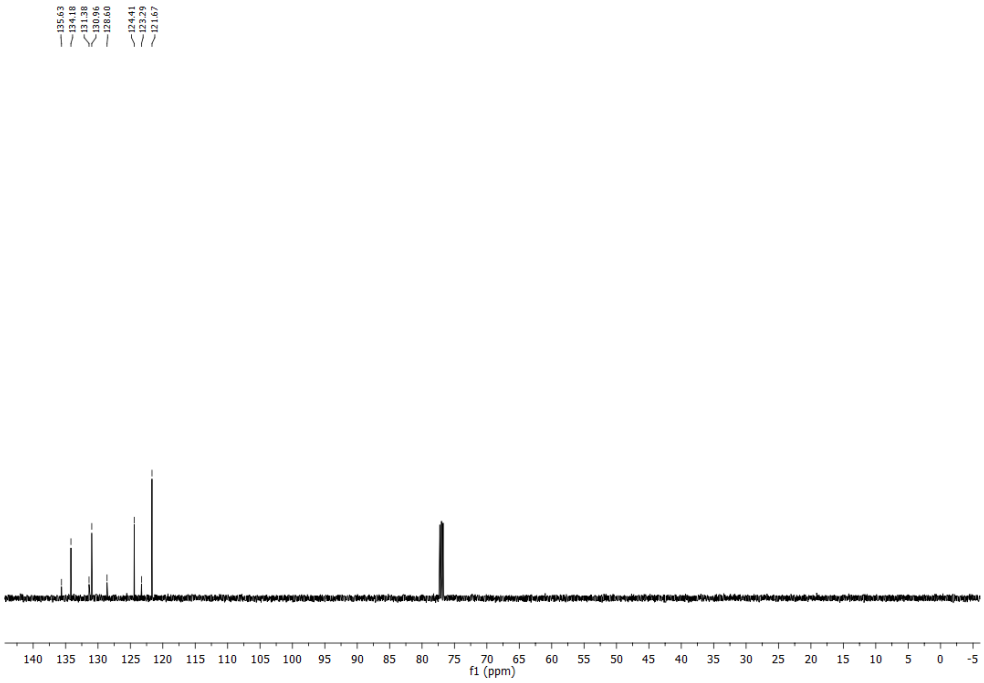

Figure S20. ^{13}C NMR spectrum of compound ***VO₂*** ($CDCl_3$, 126 MHz, 298.15 K).

IV. Mass Spectra

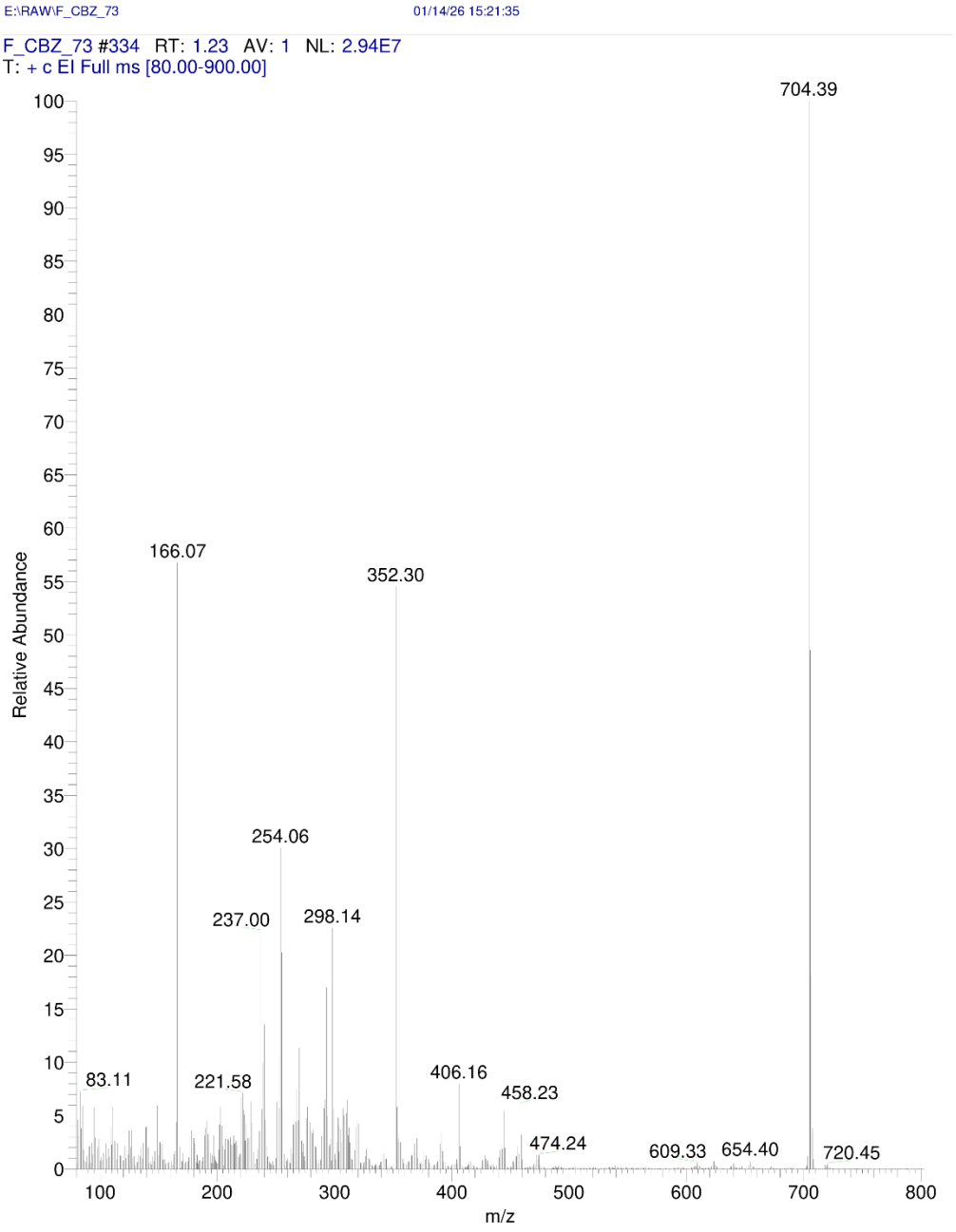

Figure S21. Mass spectrum of compound **V-CBZ$_2$**

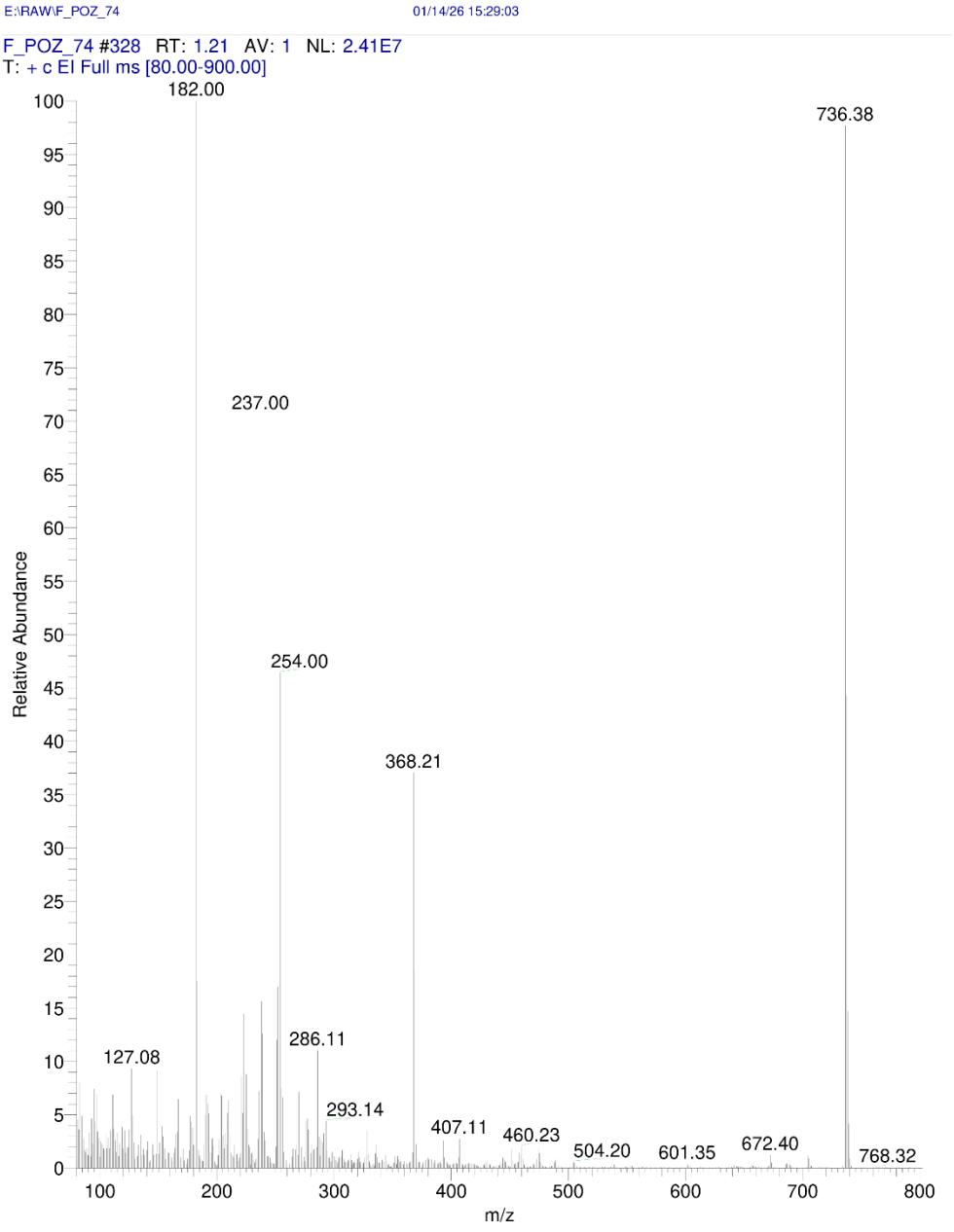

Figure S22. Mass spectrum of compound **V-POZ$_2$**

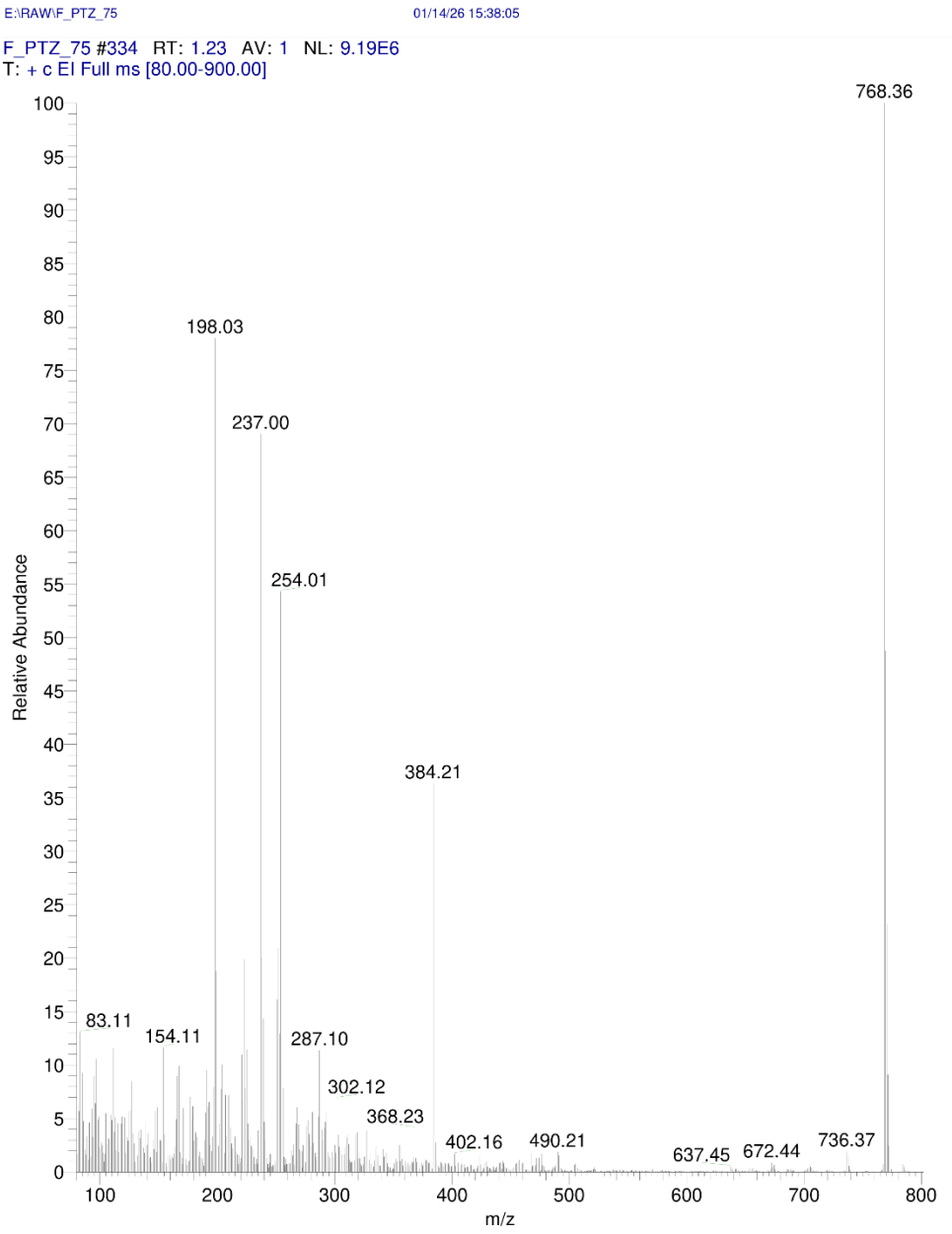

Figure S23 Mass spectrum of compound **V-PTZ$_2$**

V. Photophysical properties

Table S2. Photophysical data of **V-CBZ$_2$**, **V-POZ$_2$**, and **V-PTZ$_2$** in different solvents: Cyclohexane (CH), Toluene (TOL) and Dichloromethane (DCM).

	Solvent	λ_{abs} [nm]	λ_{PL} [nm]	Stokes shift [eV]	$PLQY_{air}$ | $PLQY_{deox}$ [%]
V-CBZ$_2$	CH	292, 311, 324, 338	455	0.94	84.3 | 100
	TOL	293, 315, 326, 339	480	1.07	86.7 | 100
	DCM	293, 315, 326, 339	533	1.33	50.3 | 68.9
V-POZ$_2$	CH	241, 322	545	1.57	8.75 | 14.2
	TOL	323	625	1.85	3.22 | 6.1
	DCM	241, 323	≈ 730	2.14	–
V-PTZ$_2$	CH	259, 318	557	1.67	2.17 | 4.3
	TOL	320	646	1.95	1.57 | 3.3
	DCM	258, 320	≈800	2.33	–

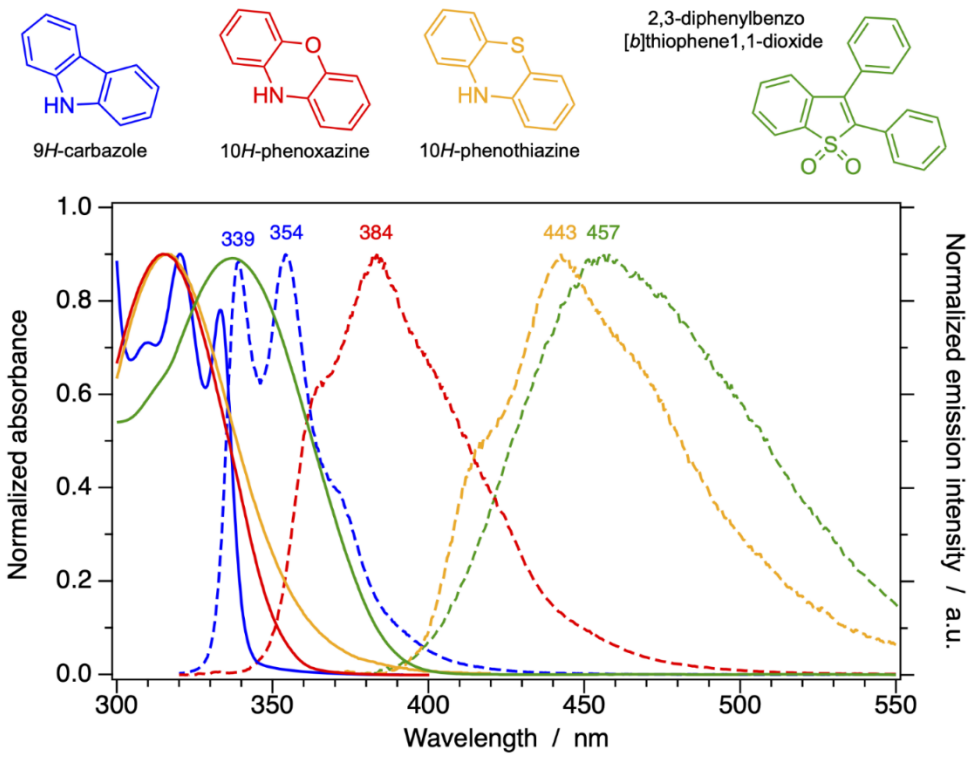

Figure S24. Normalized absorption (solid line) and emission spectra (dashed line) of the individual donor (blue, red, orange) and acceptor units (green), recorded in dichloromethane solution at 298 K.

VI. DFT calculations

Table S3. Selected geometrical parameters of the fully optimized geometries of **V-CBZ$_2$**, **V-POZ$_2$**, and **V-PTZ$_2$** in their ground state, resulting from optimizations at the CAM-B3LYP-D4/def-SVP level of theory in dichloromethane (using CPCM). Angles between the acceptor and the spacers (*i.e.*, α and α') and between each spacer and the nearby donor (*i.e.*, β and β') are computed as the angle between the two planes best fitting the atoms of each moiety. Distances between donors (D and D') and the acceptor (A) are calculated considering the centroids of each unit.

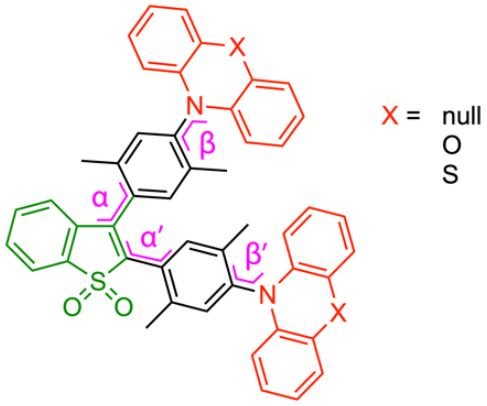

	α (°)	α' (°)	β (°)	β' (°)	d_{DA} (Å)	$d_{D'A}$ (Å)	DAD' (°)
V-CBZ$_2$	73.9	78.2	75.1	72.3	9.65	10.29	46.7
V-POZ$_2$	71.1	76.6	81.5	81.8	9.26	9.98	54.4
V-PTZ$_2$	73.4	77.8	86.9	82.0	9.19	9.91	53.4

Table S4. Lowest eight singlet vertical excitations calculated for **V-CBZ$_2$** in its ground-state geometry. Data are computed by TD-DFT (using TDA) at the CAM-B3LYP-D4/def-SVP level of theory in dichloromethane (using CPCM). Density differences ($\rho_{Sn} - \rho_{S0}$) are used to describe the nature of each transition: yellow (or pink) isosurfaces correspond to regions with a decrease (or increase) in the electron density with respect to the ground state (isovalue: 0.0005 e bohr^{-3}).

	Transition energy [eV] Oscillator strength (f)	Transition	Nature
$S_0 \rightarrow S_1$	4.36 $f = 0.216$	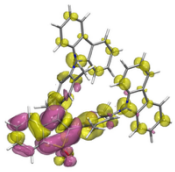	mixed charge transfer and local excitation on benzothiophene-dioxide acceptor
$S_0 \rightarrow S_2$	4.48 $f = 0.015$	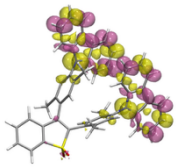	centered on the carbazole donors
$S_0 \rightarrow S_3$	4.49 $f = 0.176$	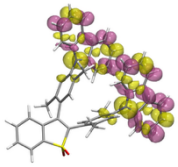	
$S_0 \rightarrow S_4$	4.63 $f = 0.091$	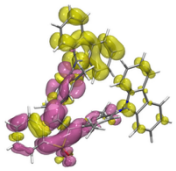	charge-transfer from the donor to the acceptor with different contributions from the spacers
$S_0 \rightarrow S_5$	4.66 $f = 0.034$	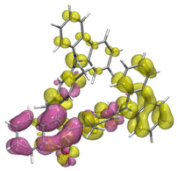	
$S_0 \rightarrow S_6$	4.86 $f = 0.033$	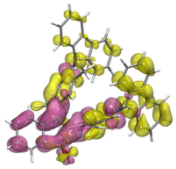	
$S_0 \rightarrow S_7$	4.92 $f = 0.457$	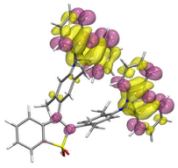	centered on the carbazole donors

$S_0 \rightarrow S_8$	4.93 $f = 0.020$	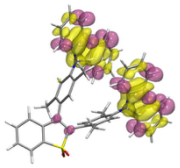

Table S5. Lowest eight singlet vertical excitations calculated for **V-POZ$_2$** in its ground-state geometry. Data are computed by TD-DFT (using TDA) at the CAM-B3LYP-D4/def-SVP level of theory in dichloromethane (using CPCM). Density differences ($\rho_{Sn} - \rho_{S0}$) are used to describe the nature of each transition: yellow (or pink) isosurfaces correspond to regions with a decrease (or increase) in the electron density with respect to the ground state (isovalue: 0.0005 e bohr^{-3}).

	Transition energy [eV] Oscillator strength (f)	Transition	Nature
$S_0 \rightarrow S_1$	3.87 $f = 0.030$	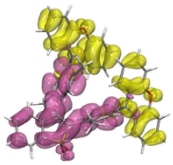	charge-transfer from the donor to spacers/acceptor
$S_0 \rightarrow S_2$	3.89 $f = 0.017$	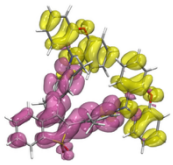	
$S_0 \rightarrow S_3$	4.02 $f = 0.044$	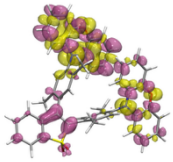	mainly centered on the phenoxazine donors
$S_0 \rightarrow S_4$	4.04 $f = 0.019$	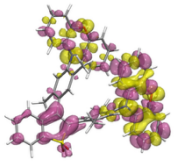	
$S_0 \rightarrow S_5$	4.37 $f = 0.151$	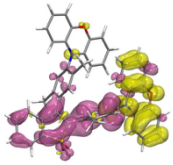	charge-transfer from the donor to the spacers/acceptor
$S_0 \rightarrow S_6$	4.40 $f = 0.178$	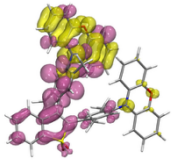	
$S_0 \rightarrow S_7$	4.41 $f = 0.131$	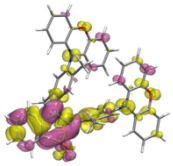	mainly centered on the benzothiophene-dioxide acceptor with partial CT character

$S_0 \rightarrow S_8$	4.49 $f = 0.201$	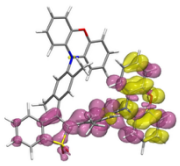	charge-transfer from the donor to the spacer

Table S6. Lowest eight singlet vertical excitations calculated for **V-PTZ$_2$** in its ground-state geometry. Data are computed by TD-DFT (using TDA) at the CAM-B3LYP-D4/def-SVP level of theory in dichloromethane (using CPCM). Density differences ($\rho_{Sn} - \rho_{S0}$) are used to describe the nature of each transition: yellow (or pink) isosurfaces correspond to regions with a decrease (or increase) in the electron density with respect to the ground state (isovalue: 0.0005 e bohr^{-3}).

	Transition energy [eV] Oscillator strength (f)	Transition	Nature
$S_0 \rightarrow S_1$	4.01 $f = 0.021$	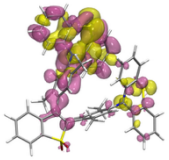	mainly centered on the phenothiazine donors with minor charge-transfer contribution to the spacers
$S_0 \rightarrow S_2$	4.01 $f = 0.009$	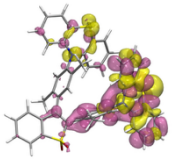	
$S_0 \rightarrow S_3$	4.26 $f = 0.019$	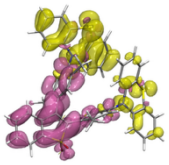	charge-transfer from the donor to spacers/acceptor
$S_0 \rightarrow S_4$	4.28 $f = 0.050$	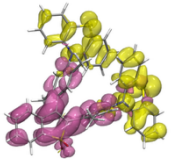	
$S_0 \rightarrow S_5$	4.43 $f = 0.177$	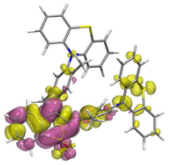	mixed charge transfer and local excitation on benzothiophene-dioxide acceptor
$S_0 \rightarrow S_6$	4.61 $f = 0.059$	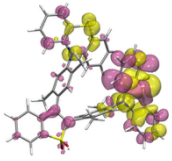	centered on the phenothiazine donors
$S_0 \rightarrow S_7$	4.61 $f = 0.036$	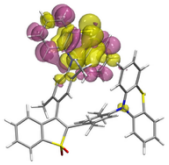	

$S_0 \rightarrow S_8$	4.62 $f = 0.097$	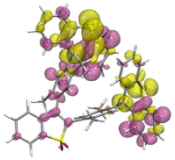	mainly centered on the phenothiazine donors with minor CT character

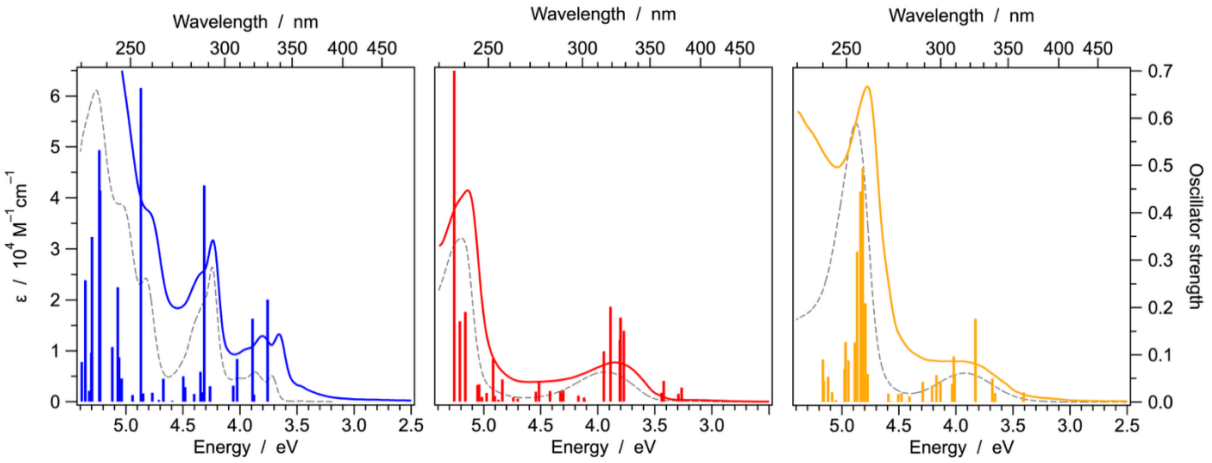

Figure S25. Comparison between the experimental absorption spectra of **V-CBZ$_2$** (blue), **V-POZ$_2$** (red), and **V-PTZ$_2$** (orange) in DCM solution at 298 K and the TD-DFT (TDA) computed excitations at the CAM-B3LYP-D4/def-SVP level of theory in dichloromethane (using CPCM). The absorption spectra of the individual donors (*i.e.*, 9*H*-carbazole, 10*H*-phenoxazine and 10*H*-phenithiazine) have also been reported for clarity (gray dashed line, ε is multiplied by a factor of 2 since there are two donor units per molecule). The energy of each TD-DFT transition is red-shifted by 0.6 eV for a better agreement with the experimental data.

a)

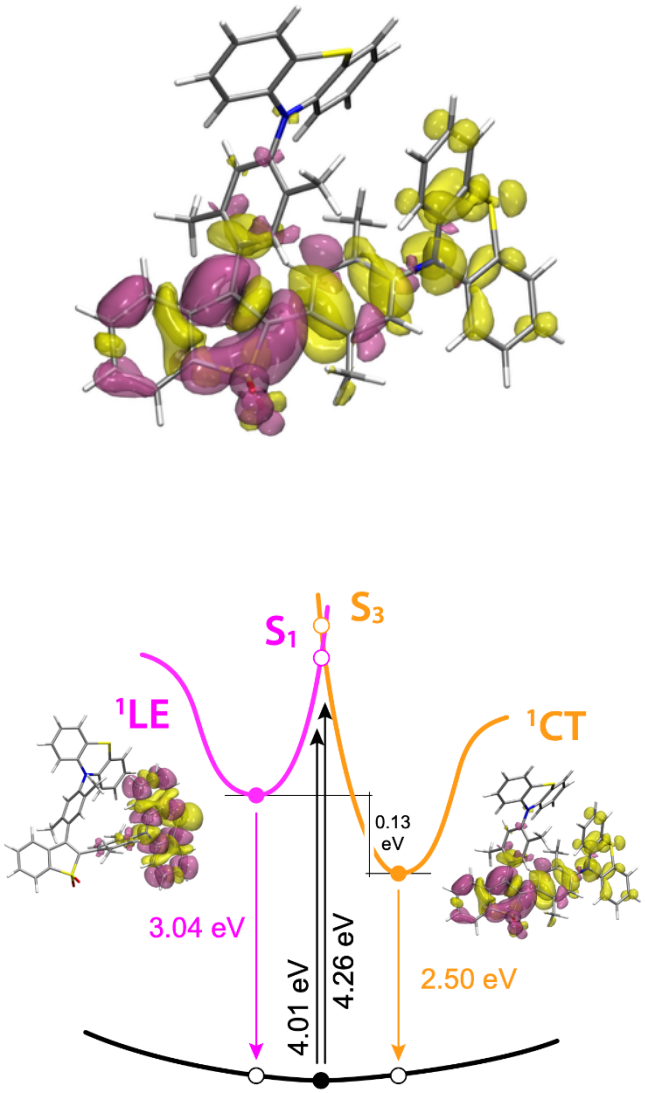

Figure S26. a) TD-DFT optimized geometry of the S_3 state (at the Franck–Condon region) of **V-PTZ$_2$** (2.50 eV above S0) in DCM, which is the lowest excited-state with a predominant charge-transfer character. Density difference ($\rho_{S3} - \rho_{S0}$) is used to describe the nature of the excited state: yellow (or pink) isosurfaces correspond to regions with a decrease (or increase) in the electron density with respect to the ground state (isovalue: 0.0005 e bohr^{-3}). b) Schematic excited-state energy diagram of **V-PTZ$_2$** in DCM computed with TD-DFT at the CAM-B3LYP-D4/def-SVP level.

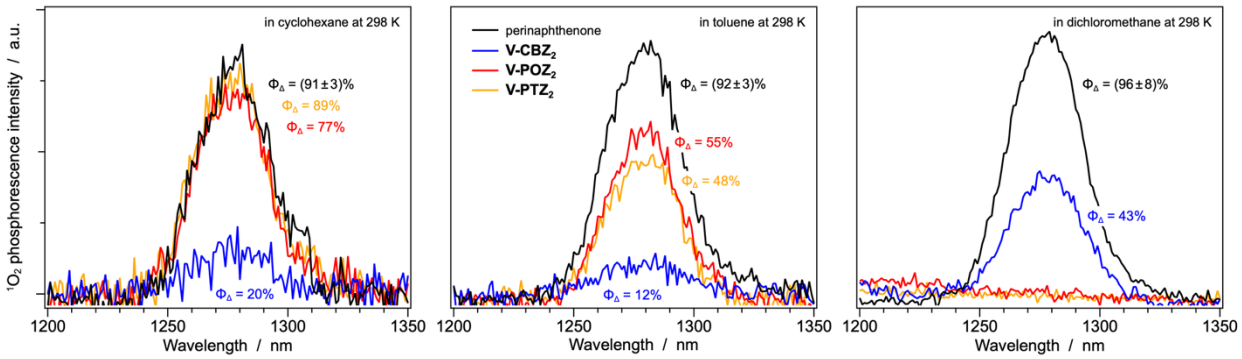

Figure S27. Singlet-oxygen phosphorescence spectra of cyclohexane, toluene, and dichloromethane solution at 298 K, containing **V-CBZ$_2$**, **V-POZ$_2$**, and **V-PTZ$_2$** with the same optical density at the excitation wavelength (A = 0.30). Samples are excited at 325 nm, using an He–Cd laser. The quantum yields of singlet oxygen production (Φ_Δ) are estimated relative to perinaphthenone, which was measured under identical experimental conditions. [*see Ref.* J. *Photochem. Photobiol. A Chem*., **1996**, 87, 11-18]

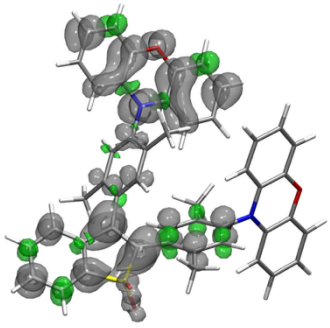

V-POZ$_2$ (CT')
ΔE_{ad} ($T_{CT'}$–S_0) = + 2.21 eV

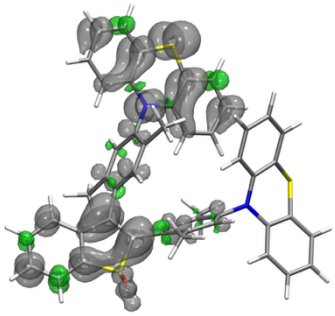

V-PTZ$_2$ (CT')
ΔE_{ad} ($T_{CT'}$–S_0) = + 2.27 eV

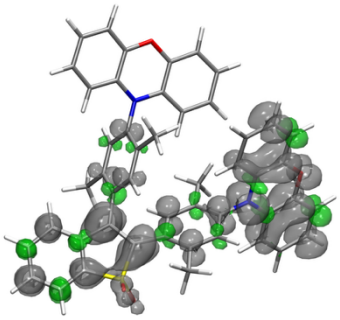

V-POZ$_2$ (CT)
ΔE_{ad} (T_{CT}–S_0) = + 2.17 eV

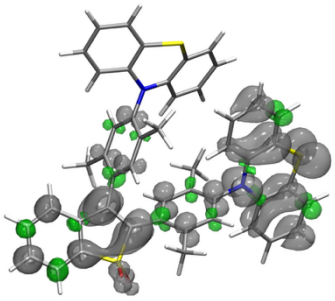

V-PTZ$_2$ (CT)
ΔE_{ad} (T_{CT}–S_0) = + 2.24 eV

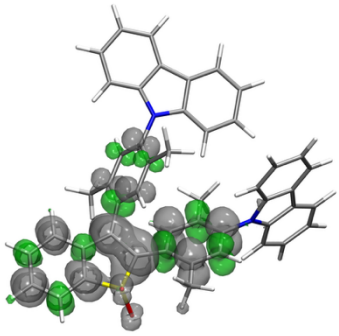

V-CBZ$_2$
ΔE_{ad} (T_{LE}–S_0) = + 2.13 eV

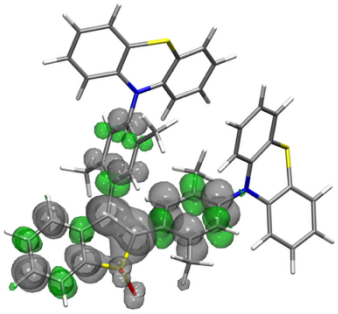

V-PTZ$_2$ (LE)
ΔE_{ad} (T_{LE}–S_0) = + 2.14 eV

Figure S28. Spin-density distribution of the lowest triplet states, having different natures, of **V-CBZ$_2$**, **V-POZ$_2$**, and **V-PTZ$_2$** in their fully-optimized geometry, resulting from optimizations at the CAM-B3LYP-D4/def-SVP level of theory, computed in dichloromethane (isovalues: 0.002 e bohr^{-3}). The adiabatic energy difference between S_0 and T_1 is also reported (*i.e.*, ΔE_{ad}).

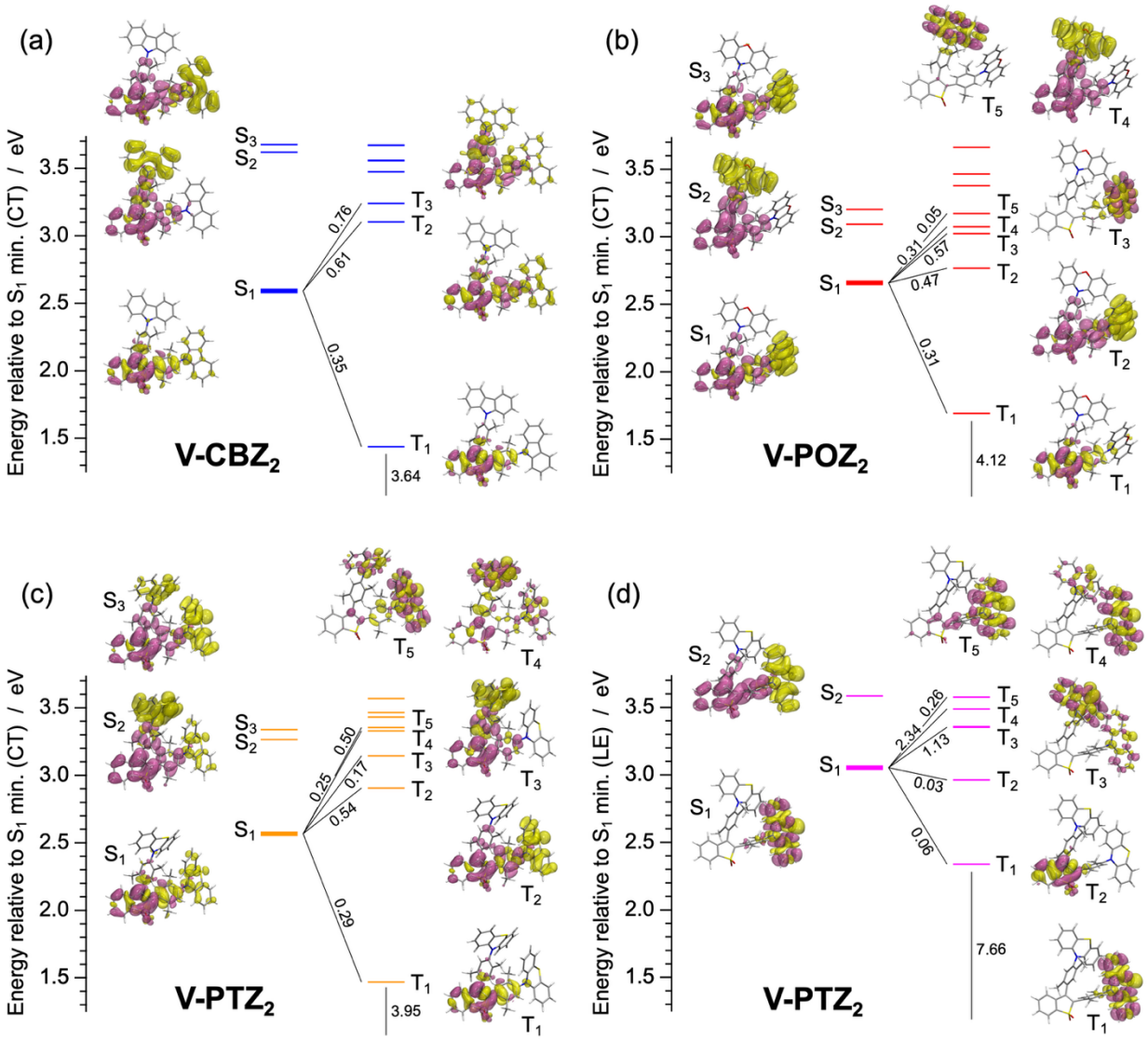

Figure S29. Excited-state scenario, calculated at the TD-CAM-B3LYP-D4/def2-SVP level of theory in dichloromethane (CPCM), for **V-CBZ$_2$** (a), **V-POZ$_2$** (b), and **V-PTZ$_2$** (c and d, for the CT and LE state, respectively) in their fully optimized S_1 geometry. Spin–orbit coupling matrix elements between S_1 and relevant triplet states, as well as between T_1 and S_0, are reported (in cm^{-1}) to provide insight into the experimentally relevant intersystem crossing processes.

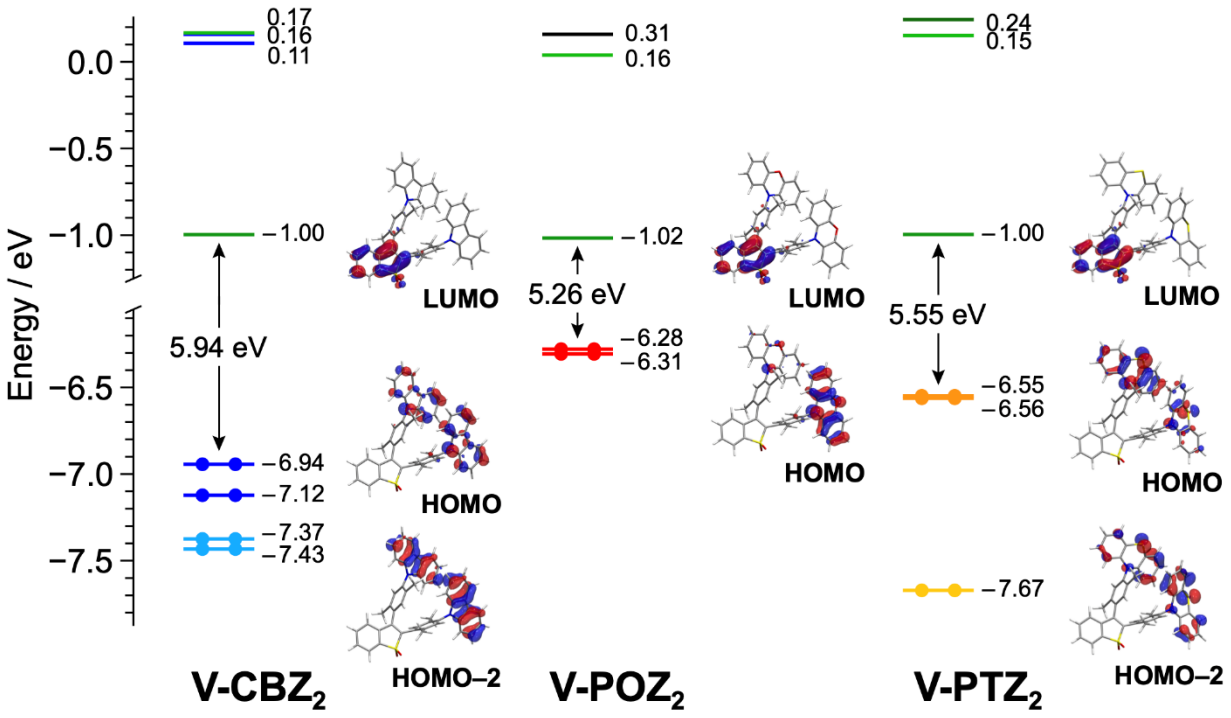

Figure S30. Energy diagram showing the frontier molecular orbitals of **V-CBZ$_2$**, **V-POZ$_2$**, and **V-PTZ$_2$** in dichloromethane. For some relevant orbitals, the corresponding isosurface is also displayed (isovalues = 0.04 $e^{1/2}$ $bohr^{-3/2}$). Along the series, relevant orbitals with similar topologies are plotted with the same colour for an easier comparison.

VII. Electrochemical characterization

Table S7. Redox potentials of **V-CBZ$_2$**, **V-POZ$_2$**, and **V-PTZ$_2$** in acetonitrile solution (1.0 mM) + 0.1 M $TBAPF_6$ at 298 K vs. the ferrocene/ferrocenium couple, used as an internal reference.

	Cyclic voltammetry	
	E_{ox} [V]	E_{red} [V]
V-CBZ$_2$	+ 0.89	– 1.916
V-POZ$_2$	+ 0.340	– 1.911
V-PTZ$_2$	+ 0.319	– 1.908

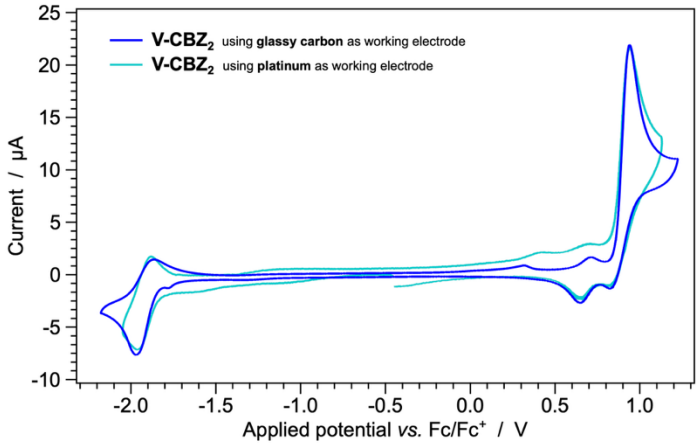

Figure S31. CVs of **V-CBZ$_2$**, in acetonitrile solution at 298 K (sample concentration: 1.0 mM) using either glassy carbon or platinum as working electrode.

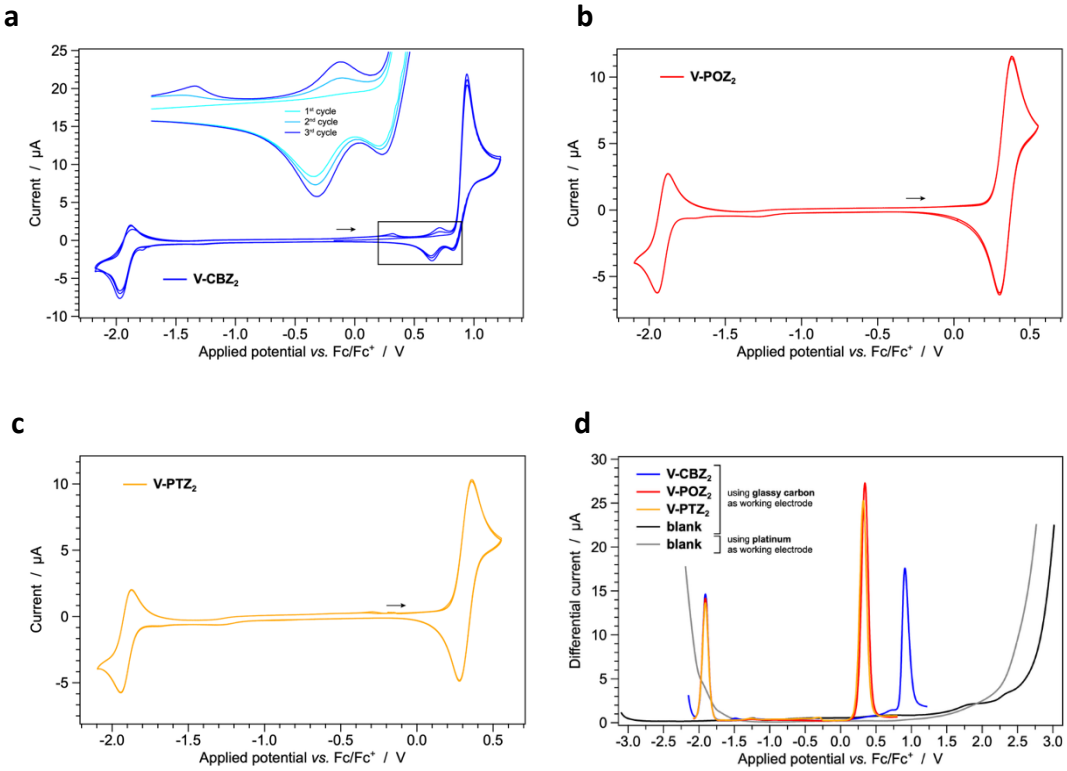

Figure S32. Three-cycle CVs at 100 mV s^{-1} in acetonitrile solution at 298 K with 1.0 mM sample concentration and 0.1 M $TBAPF_6$ supporting electrolyte (a-c). Square-wave voltammetry (SWV) measurements of investigated samples and e pure acetonitrile/$TBAPF_6$ electrolyte solution across the entire potential window used in our experiments (d); scan rate of 25 mV s^{-1}, SW amplitude of ± 20 mV, and a frequency of 25 Hz.

VIII. Thin film characterizations

Table S8. Photophysical data of **V-CBZ$_2$**, **V-POZ$_2$**, and **V-PTZ$_2$** in PMMA and neat film.

molecule	form	λ_{PL} [nm]	$PLQY^{air}/PLQY^{deox}$ [%]	τ [ns]	τ [μs]
V-CBZ$_2$	PMMA	455	40.7/48.5	λ_{em}=450 nm 4.7(39%); 9.7 (61%)	-
	Neat film	481	37.0/57.2	λ_{em}=475 nm 2.3(10%); 6.3 (62%); 16.1 (28%)	-
V-POZ$_2$	PMMA	562	5.6/13.1	λ_{em}=540 nm 7.1(30%); 20.1(70%)	-
	Neat film	602	2.6/5.3	λ_{em}=570 nm 2.1(5%); 10.9(54%); 25.5(41%)	λ_{em}=570 nm 7.6(47%); 23.7(53%) τ_{av}=20.1
V-PTZ$_2$	PMMA	593	1.4/1.7	λ_{em}=550 nm 1.8(9%); 7.8(47%); 18.7(44%)	λ_{em}=580 nm 12.1(42%); 86.2(58%) τ_{av}=79.3
	Neat film	632	2.0/3.1	λ_{em}=590 nm 1.4(2%); 9.8(41%); 27.4(58%)	λ_{em}=590 nm 8.1(32%); 29.4(68%) τ_{av}=26.9

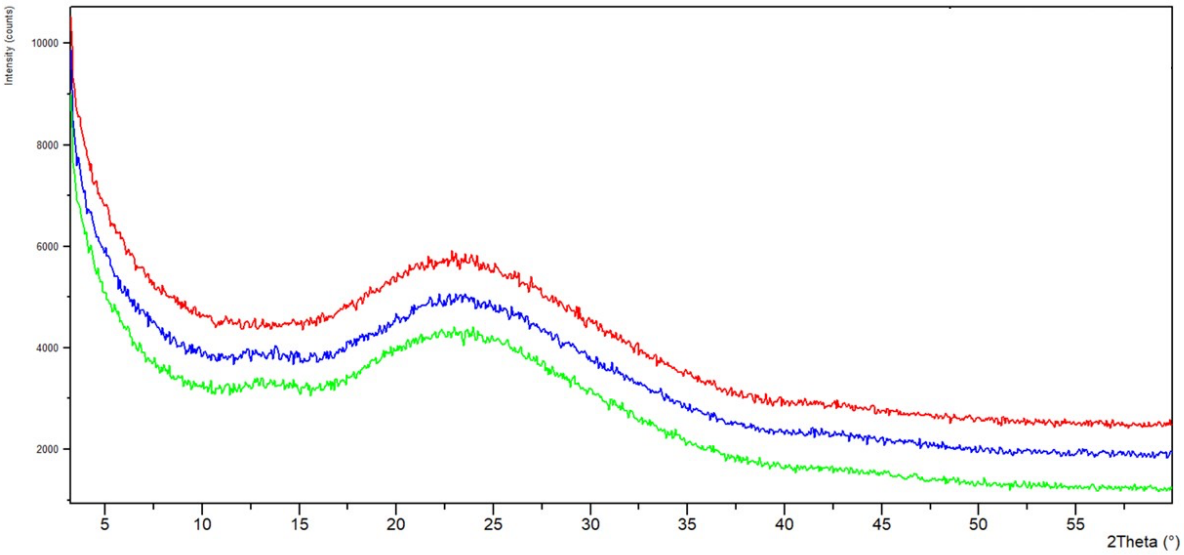

Figure S33. XRD profiles of thin films of **V-CBZ$_2$** (red), **V-POZ$_2$** (blue), and **V-PTZ$_2$** (green) deposited from toluene solutions.

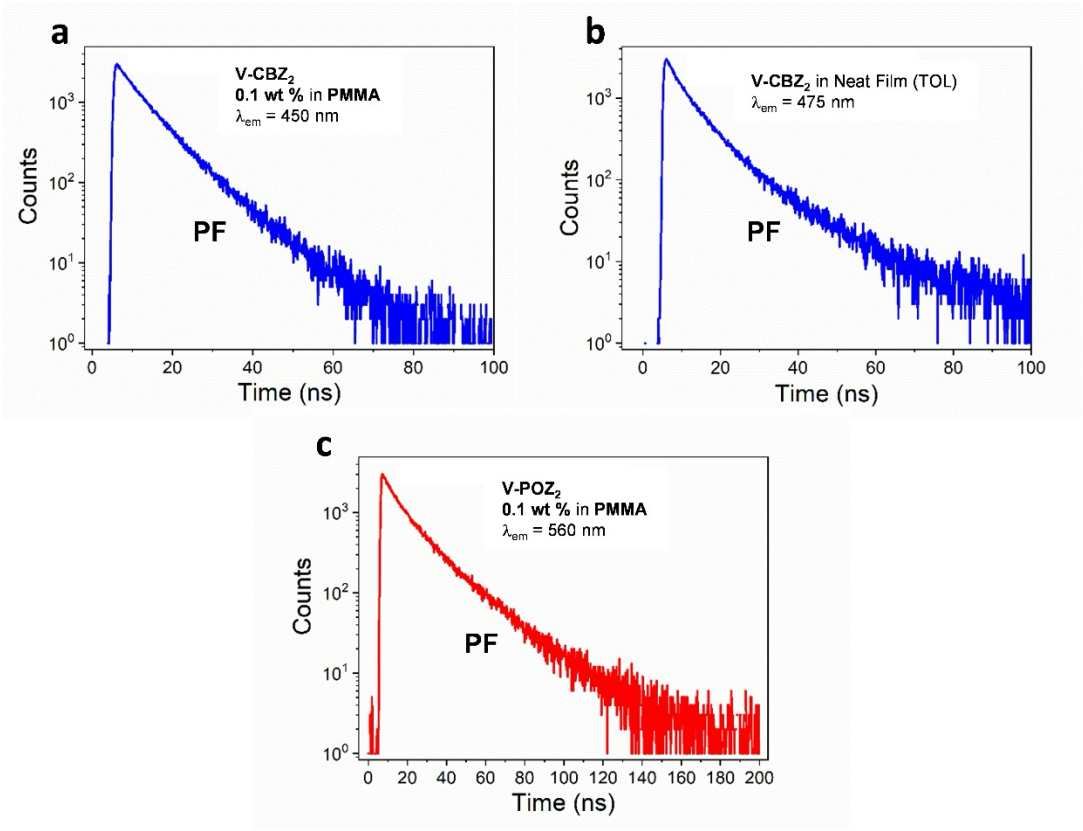

Figure S34. PL decay of (a) **V-CBZ$_2$** in PMMA (0.1 wt%) (b) **V-CBZ$_2$** neat film (c) **V-POZ$_2$** in PMMA (0.1 wt%).

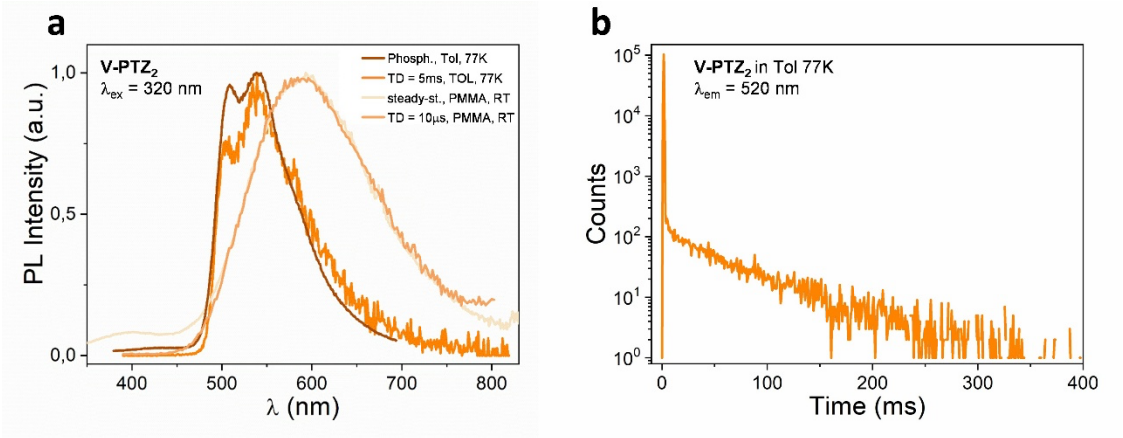

Figure S35. a) steady state and delayed PL emission of **V-PTZ$_2$** in PMMA (RT) compared with the phosphorescence spectrum of **V-PTZ$_2$** (77 K) vs. **PTZ** (77 K). b) Photoluminescence decay of **V-PTZ$_2$** at 77 K.

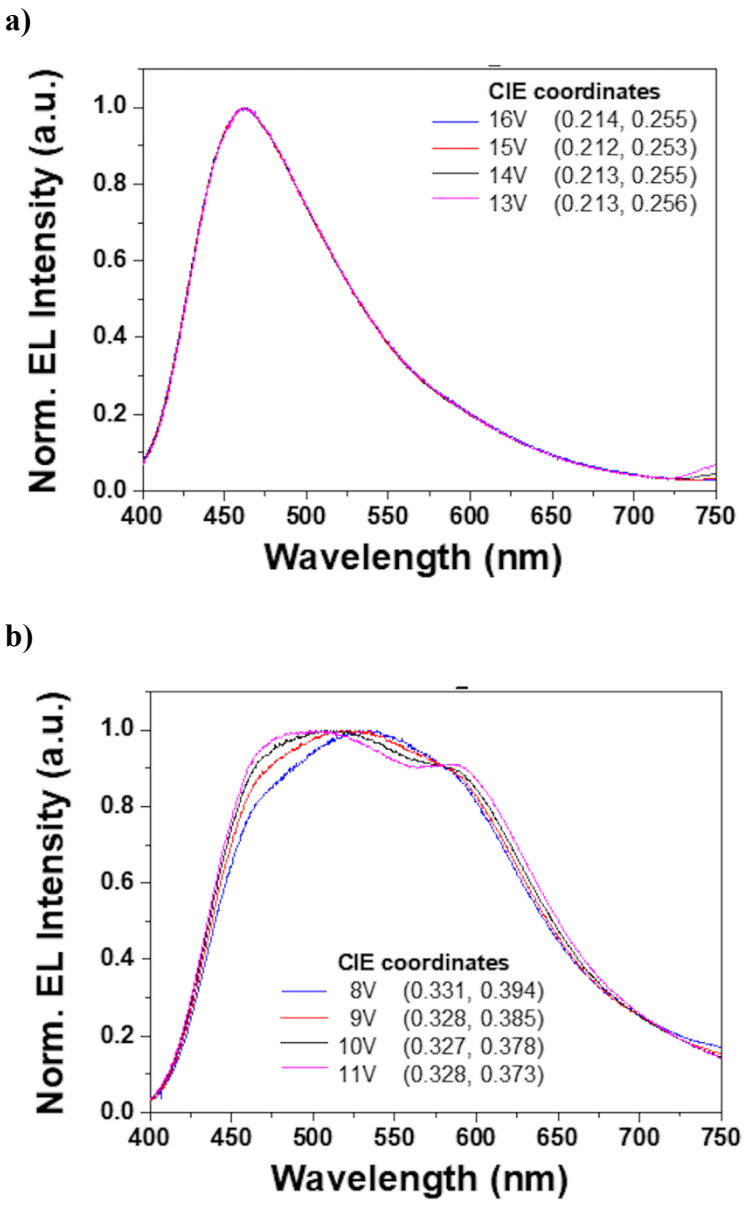

Figure S36. EL Spectra at different working voltages of (a) PVK/DPEPO:**V-CBZ$_2$** (15%)-based and (b) PVK/**V-CBZ$_2$**-based electroluminescent devices.

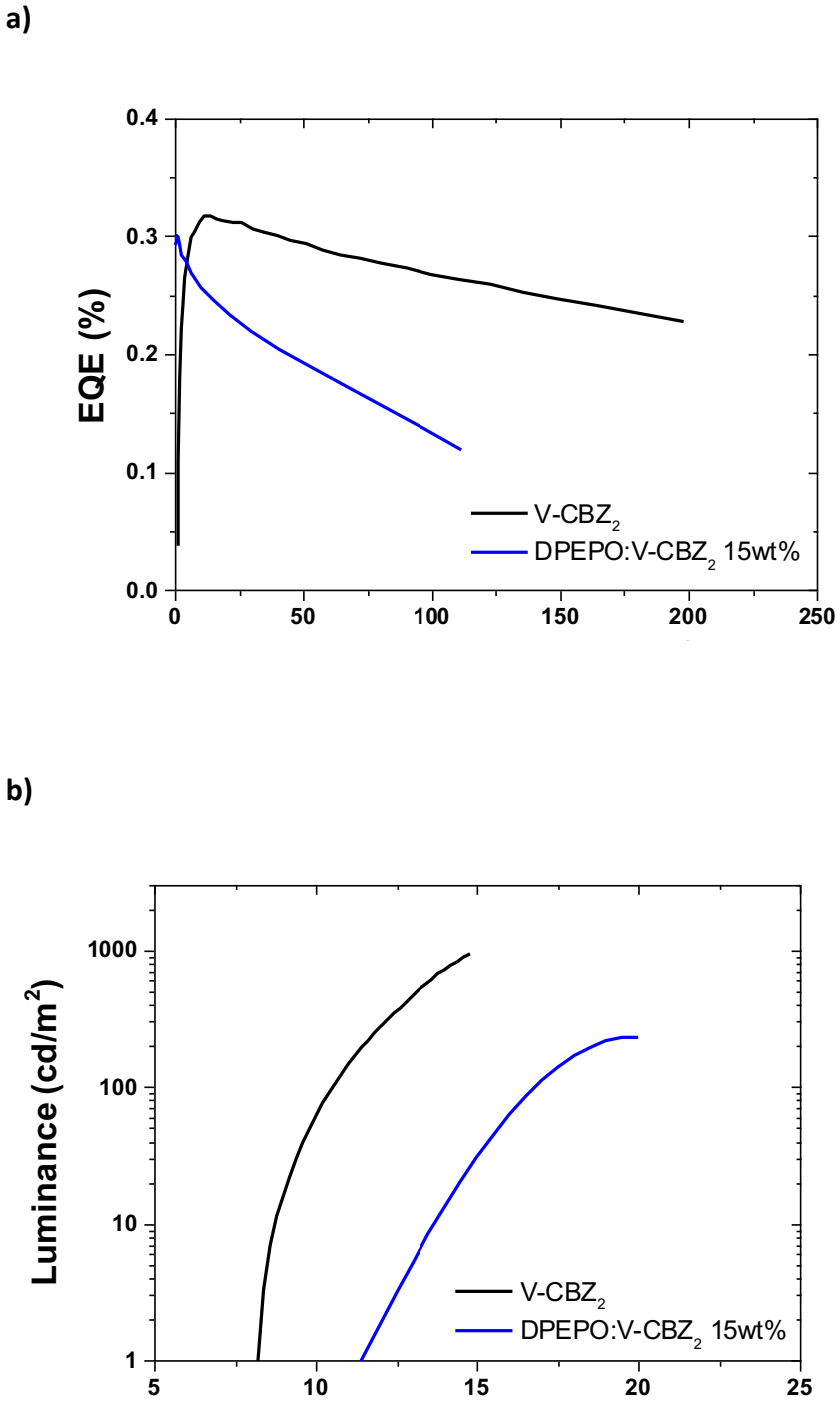

Figure S37. a) External Quantum Efficiency (EQE) vs Current Density curves of the fabricated OLEDs. b) Luminance Vs Voltage curves of the fabricated OLEDs. At 1 cd/m^2 the **V-CBZ$_2$** and DPEPO:**V-CBZ$_2$**-based devices show a turn on voltage of 8.2 V, and 11.4 V, respectively.